
Transformers Provably Implement In-Context Reinforcement Learning with Policy Improvement

Haodong Liang, Lifeng Lai
Department of Electrical and Computer Engineering
University of California, Davis
{hdlang, lflai}@ucdavis.edu

Abstract

We investigate the ability of transformers to perform in-context reinforcement learning (ICRL), where a model must infer and execute learning algorithms from trajectory data without parameter updates. We show that a linear self-attention transformer block can provably implement policy-improvement methods, including semi-gradient SARSA and actor-critic, via explicit parameter constructions. Beyond existence, we design a teacher-mimicking training procedure, analyze its gradient-flow dynamics, and establish the first convergence guarantee in the ICRL literature: under suitable richness conditions on the training MDP distribution, gradient flow converges locally and exponentially to an optimal parameter manifold corresponding to the desired RL update. Empirically, training transformers on randomly generated tabular MDPs confirms these predictions: the learned models recover the parameter structure of our explicit constructions and, when deployed on unseen MDPs, deliver strong in-context control performance. Together, these results illuminate how transformer architectures internalize and execute classical reinforcement learning algorithms in context, bridging mechanistic understanding and training dynamics in ICRL.

1 Introduction

In-context learning (ICL) refers to a model’s ability to learn and perform a new task by conditioning on examples provided in its input, without any parameter updates [Brown et al., 2020, Garg et al., 2022, Dong et al., 2024]. The transformer architecture [Vaswani et al., 2017] has empirically demonstrated remarkable in-context learning capabilities across a wide range of tasks, among which Large Language Models (LLMs) are the most prominent example [Brown et al., 2020, Chowdhery et al., 2023, OpenAI et al., 2024].

This phenomenon has motivated substantial interest in understanding the mechanisms that enable transformers to learn in-context. A growing body of theoretical work has sought to understand this by asking: *which algorithms can a transformer execute in context, and why can it implement them?*

For supervised learning problems, this question now has a fairly complete answer: trained transformers can be shown to implement variants of gradient descent and closed-form least squares on the in-context examples, with explicit constructions and, in special cases, end-to-end training-dynamics guarantees [Garg et al., 2022, von Oswald et al., 2023, Akyürek et al., 2023, Ahn et al., 2023, Mahankali et al., 2024, Bai et al., 2023, Zhang et al., 2024, Liang et al., 2025].

Beyond the supervised learning scenario, recent works have begun to extend this lens to in-context reinforcement learning (ICRL)[Laskin et al., 2023, Lin et al., 2024, Moeini et al., 2025], where an agent is given a trajectory in its context and must internally execute a policy evaluation or policy improvement step — core operations in the reinforcement learning framework [Sutton and Barto, 2018]. A central question in this line of work is:

*Can a transformer block implement – and be trained to implement
standard RL algorithms such as temporal-difference (TD) methods, SARSA, or actor-critic?*

While these works, including Laskin et al. [2023], Lee et al. [2023], Brooks et al. [2023], and Rapparth et al. [2023], primarily focus on empirical experiments and demonstrate strong performance in various ICRL settings, they lack theoretical guarantees on the underlying mechanisms. Toward a theoretical answer, Wang et al. [2025] take a first step by showing that a linear-attention block admits a closed-form structure that implements policy evaluation via TD learning. Two questions, however, remain open. First, their analysis is restricted to policy evaluation, leaving open whether a transformer can also implement *policy-improvement* algorithms – a component that is no less central to RL. Second, existing analyses establish only the existence of an *invariant* set: once the parameters lie in the set, the expected update keeps them there. They do not show whether the training actually drives the parameters into this set in the first place, nor identify the conditions under which it does.

In this work, we close both gaps: we move from policy evaluation to *policy improvement* by showing that a single linear-attention block can implement classical on-policy control updates – SARSA and actor-critic – and we move from invariance to *convergence* by identifying sufficient conditions under which gradient training provably drives the transformer parameters into the theoretical manifold that exactly realizes the target update.

Our existence theorem is similar in form to Wang et al. [2025] in that both exhibit a closed-form weight configuration $(\mathbf{P}^*, \mathbf{V}^*)$ for a single linear-attention block, but there are substantial differences. In Wang et al. [2025], their transformer outputs only the value estimate at the query sample, so the construction is tailored to a fixed policy evaluation problem and cannot be reused to drive further interaction. Our construction instead directly outputs the updated parameters themselves – the critic parameter \mathbf{w} for SARSA, and both the critic \mathbf{w} and the actor $\boldsymbol{\lambda}$ for actor-critic – which can then be utilized to update policy, sample new trajectories, and close the in-context policy-improvement loop.

On the training-dynamics side, the optimum is no longer a single point but a continuous manifold of equivalent constructions, so global strong-convexity arguments do not apply directly; we instead establish a *local* Polyak–Łojasiewicz inequality on a tubular neighborhood of the manifold which, together with explicit richness conditions on the training-MDP distribution, yields exponential convergence of the gradient flow to a single point on the manifold.

Our contributions are summarized as follows:

- **Existence Proof.** We construct explicit parameters $\boldsymbol{\theta}^* = (\mathbf{P}^*, \mathbf{V}^*)$ for a single-head linear self-attention block such that $\text{TF}_{\boldsymbol{\theta}^*}$ exactly realizes the batch SARSA semi-gradient update (Theorem 3.1) and the batch actor-critic update (Theorem 3.3).
- **Local convergence.** Under explicit richness assumptions on the training-MDP distribution (Assumption 1), we prove that by mimicking the teacher updates, the gradient flow on the population loss converges locally to a single point on the manifold (Theorem 3.2). To our knowledge this is the first convergence guarantee in the ICRL literature.
- **Empirical validation.** We design ICRL training algorithms (Algorithm 1, Algorithm 2) for both the SARSA and actor-critic settings, and show that the resulting trained transformers recover the theoretical block structure of the attention parameters $(\mathbf{P}^*, \mathbf{V}^*)$ (Section 4.1). Furthermore, when deployed on unseen MDPs, the trained transformers closely track their analytical teachers and drive policies toward oracle-level returns (Section 4.2).

Additional related work: We provide a detailed discussion of more related work in Appendix A.

2 Preliminaries

2.1 Transformer architecture

We consider a one-layer, single-head, linear-attention transformer block with parameters $\boldsymbol{\theta} = \{(\mathbf{P}, \mathbf{V})\} \subseteq \mathbb{R}^{D \times D}$. Given input $\mathbf{H} \in \mathbb{R}^{D \times n}$, the output of the attention layer is given by

$$\mathbf{H}_{\text{out}} := \mathbf{H} + \frac{1}{n}(\mathbf{V}\mathbf{H})(\mathbf{H}^\top \mathbf{P}\mathbf{H}) \in \mathbb{R}^{D \times n}, \quad (1)$$

where $\mathbf{P} := \mathbf{Q}^\top \mathbf{K}$ absorbs the query and key projections. The transformer output is given by $\text{TF}_{\boldsymbol{\theta}}(\mathbf{H}) := f_{\text{read}}(\mathbf{H}_{\text{out}})$ for a fixed readout $f_{\text{read}} : \mathbb{R}^{D \times n} \rightarrow \mathbb{R}^{D_{\text{out}}}$.

2.2 Markov decision process

A Markov decision process (MDP) is a tuple $(\mathcal{S}, \mathcal{A}, P, R, \gamma)$ with state space \mathcal{S} , action space \mathcal{A} , transition kernel $P : \mathcal{S} \times \mathcal{A} \rightarrow \mathcal{P}(\mathcal{S})$, reward $R : \mathcal{S} \times \mathcal{A} \rightarrow \mathbb{R}$, and discount $\gamma \in [0, 1)$, where $\mathcal{P}(\mathcal{X})$ denotes the set of probability distributions over \mathcal{X} . The goal is to find a policy $\pi : \mathcal{S} \rightarrow \mathcal{P}(\mathcal{A})$ maximizing the (expected) return $G_t := \sum_{k=0}^{\infty} \gamma^k r_{t+1+k}$. The state- and action-value functions under π are

$$v_\pi(s) := \mathbb{E}_\pi[G_t \mid s_t = s], \quad q_\pi(s, a) := \mathbb{E}_\pi[G_t \mid s_t = s, a_t = a].$$

2.3 SARSA

SARSA is an on-policy value-based algorithm. Given a feature map $\phi : \mathcal{S} \times \mathcal{A} \rightarrow \mathbb{R}^d$ and parameter $\mathbf{w} \in \mathbb{R}^d$, we consider linear function approximation $q_\mathbf{w}(s, a) = \mathbf{w}^\top \phi(s, a)$, and the batch semi-gradient SARSA update over an n -step trajectory is

$$\mathbf{w}_{\text{SARSA}} = \mathbf{w} + \frac{\alpha}{n} \sum_{i=0}^{n-1} [r_{i+1} + \gamma \mathbf{w}^\top \phi(s_{i+1}, a_{i+1}) - \mathbf{w}^\top \phi(s_i, a_i)] \phi(s_i, a_i), \quad (2)$$

where $\alpha > 0$ is the step size and the bracketed quantity is the temporal-difference (TD) error.

2.4 Actor-Critic

Actor-Critic combines a parametric policy (the actor) and a parametric value function (the critic). Given a policy feature map $\phi_\pi : \mathcal{S} \times \mathcal{A} \rightarrow \mathbb{R}^m$, a value feature map $\phi_V : \mathcal{S} \rightarrow \mathbb{R}^d$, and parameters $\lambda \in \mathbb{R}^m$, $\mathbf{w} \in \mathbb{R}^d$, with softmax policy $\pi_\lambda(a \mid s) \propto \exp(\lambda^\top \phi_\pi(s, a))$ and linear critic $v_\mathbf{w}(s) = \mathbf{w}^\top \phi_V(s)$, the batch update over an n -step trajectory is

$$\begin{aligned} \mathbf{w}_{\text{AC}} &= \mathbf{w} + \frac{\beta}{n} \sum_{i=0}^{n-1} [r_{i+1} + \gamma \mathbf{w}^\top \phi_V(s_{i+1}) - \mathbf{w}^\top \phi_V(s_i)] \phi_V(s_i), \\ \lambda_{\text{AC}} &= \lambda + \frac{\alpha}{n} \sum_{i=0}^{n-1} \gamma^i [r_{i+1} + \gamma \mathbf{w}^\top \phi_V(s_{i+1}) - \mathbf{w}^\top \phi_V(s_i)] \mathbf{g}_\lambda(s_i, a_i), \end{aligned} \quad (3)$$

where $\alpha, \beta > 0$ are step sizes, and $\mathbf{g}_\lambda(s, a) := \phi_\pi(s, a) - \sum_b \phi_\pi(s, b) \pi_\lambda(b \mid s)$ is the score function.

3 Main Results

We demonstrate that a single-head transformer block can learn to perform in-context policy improvement using classical on-policy RL algorithms. Figure 1 illustrates the ICRL pipeline. Given a formulated input prompt $\mathbf{H}(z)$ constructed from the training sample z , we show that there exists θ^* such that the transformer block TF_{θ^*} directly outputs the updated parameter \mathbf{w} , which is then used to update the value function or policy. In Section 3.1 we establish the existence of such implementations of SARSA, and in Section 3.2 we analyze the training dynamics of the proposed training procedure and identify sufficient conditions for convergence to the optimum parameter manifold. We then extend these results to actor-critic in Section 3.3.

3.1 Transformers can implement SARSA

Let $z = (\mathcal{M}, \phi, \mathbf{w}, \tau)$ denote a training sample, where \mathcal{M} is the training MDP task, $\phi : \mathcal{S} \times \mathcal{A} \rightarrow \mathbb{R}^d$ is the feature map, $\mathbf{w} \in \mathbb{R}^d$ is the parameter of the behavior policy π , and $\tau = (s_0, a_0, r_1, \dots, s_n, a_n)$ is the resulting n -step trajectory in \mathcal{M} . For notational convenience, we define the following quantities for $i = 0, \dots, n-1$:

$$\begin{aligned} \phi_i &:= \phi(s_i, a_i) \in \mathbb{R}^d, \quad \phi_i^+ := \phi(s_{i+1}, a_{i+1}) \in \mathbb{R}^d, \quad \delta_i := r_{i+1} + \gamma \mathbf{w}^\top \phi_i^+ - \mathbf{w}^\top \phi_i \in \mathbb{R}, \\ \mathbf{x}_i &:= \begin{bmatrix} \phi_i \\ \gamma \phi_i^+ \\ r_{i+1} \end{bmatrix} \in \mathbb{R}^{2d+1}, \quad \tilde{\mathbf{w}} := \begin{bmatrix} 1 \\ \mathbf{w} \end{bmatrix} \in \mathbb{R}^{d+1}. \end{aligned}$$

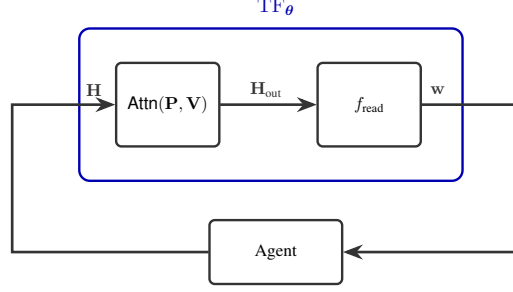


Figure 1: A simplified pipeline of transformer’s ICRL implementation. The agent samples a trajectory under the current policy, which is fed into the transformer block. The transformer outputs an updated parameter \mathbf{w} , which is then used to update the value function and policy.

We also define the following trajectory statistics:

$$\hat{\Sigma}(z) := \frac{1}{n} \sum_{i=0}^{n-1} \mathbf{x}_i \mathbf{x}_i^\top, \quad \mathbf{R}(z) := \frac{1}{n} \sum_{i=0}^{n-1} \phi_i \mathbf{x}_i^\top, \quad \mathbf{b}(z) := \frac{1}{n} \sum_{i=0}^{n-1} \mathbf{x}_i \delta_i.$$

Consider the training prompt as follows:

$$\mathbf{H}(z) = \begin{bmatrix} \mathbf{x}_0 & \cdots & \mathbf{x}_{n-1} & \mathbf{0} \\ \mathbf{0} & \cdots & \mathbf{0} & \tilde{\mathbf{w}} \end{bmatrix} \in \mathbb{R}^{D \times (n+1)}, \quad (4)$$

where $D = 3d + 2$. We now establish the existence of a transformer block that implements the batch semi-gradient SARSA update (2).

Theorem 3.1 (Implement semi-gradient SARSA with a transformer block). *Let the output projection function be $f_{\text{read}}(\cdot) = \cdot_{-d, -1}$, which extracts the last d elements of the last column. Given formulated input prompt (4), for any fixed $\alpha > 0$, there exists $\theta^* = \{(c\mathbf{P}^*, c^{-1}\mathbf{V}^*)\} \subseteq \mathbb{R}^{D \times D}$, where $c \neq 0$ and*

$$\mathbf{P}^* = \begin{bmatrix} *_{(2d+1) \times (2d+1)} & \begin{bmatrix} \mathbf{0}_{d \times 1} & -\mathbf{I}_d \\ \mathbf{0}_{d \times 1} & \mathbf{I}_d \\ 1 & \mathbf{0}_{1 \times d} \end{bmatrix} \\ *_{(d+1) \times (2d+1)} & \mathbf{0}_{(d+1) \times (d+1)} \end{bmatrix}, \quad \mathbf{V}^* = \begin{bmatrix} *_{(2d+1) \times (2d+1)} & *_{(2d+1) \times (d+1)} \\ \begin{bmatrix} *_{1 \times d} & *_{1 \times d} & * \\ \alpha \mathbf{I}_d & \mathbf{0}_{d \times d} & \mathbf{0}_{d \times 1} \end{bmatrix} & \begin{bmatrix} *_{1 \times (d+1)} \\ \mathbf{0}_{d \times (d+1)} \end{bmatrix} \end{bmatrix}, \quad (5)$$

such that transformer $TF_{\theta^*}(\mathbf{H}(z))$ directly implements batch semi-gradient SARSA update (2).

The proof is deferred to Appendix E. Theorem 3.1 guarantees the existence of a parameter configuration θ^* that realizes the semi-gradient SARSA update, but does not prescribe how to obtain it. To bridge this gap, we need to develop a training algorithm.

3.2 Algorithm and training dynamics analysis

We now design an ICRL algorithm to train the transformer to implement SARSA, as outlined in Algorithm 1. This procedure is inspired by Laskin et al. [2023]. At each iteration, trajectory data are sampled from the MDP, the corresponding SARSA update is computed as a target, and the transformer parameters are updated to minimize the discrepancy between the transformer’s prediction and the target update. The empirical loss at each step approximates the population loss defined below:

$$\mathcal{L}(\theta) = \mathbb{E}_z \left[\frac{1}{2} \left\| TF_{\theta}(\mathbf{H}(z)) - \mathbf{w}_{\text{SARSA}}(z) \right\|^2 \right], \quad (6)$$

where $\mathbf{w}_{\text{SARSA}}(z)$ is the target parameter given by the batch semi-gradient SARSA update (2). We now analyze the training dynamics under this loss objective.

We consider gradient flow, which captures the behavior of gradient descent with infinitesimal step size, and is described by the following ordinary differential equation (ODE):

$$\frac{d\theta(t)}{dt} = -\nabla \mathcal{L}(\theta(t)). \quad (7)$$

We first identify the invariant parameter groups during training.

Algorithm 1 IC-SARSA Transformer Training

- 1: **Input:** Transformer parameter $\theta^{(0)} = (\mathbf{P}^{(0)}, \mathbf{V}^{(0)})$, trajectory window length n , number of frames per MDP T , number of MDPs K , ϵ -greedy parameter ϵ , learning rate η , and SARSA step size α
 - 2: **for** $k = 0, \dots, K - 1$ **do**
 - 3: Sample a MDP $\mathcal{M}^{(k)} = (\mathcal{S}, \mathcal{A}, P^{(k)}, R^{(k)}, \gamma^{(k)})$, and generate corresponding feature map $\phi^{(k)} : \mathcal{S} \times \mathcal{A} \rightarrow \mathbb{R}^d$. Initialize parameter $\mathbf{w}^{(0)}$ and state $s_0^{(0)}$ randomly
 - 4: **for** $t = 0, \dots, T - 1$ **do**
 - 5: Estimate state-action value function $Q_{\mathbf{w}^{(t)}}^{(k)}(s, a) = \mathbf{w}^{(t)\top} \phi^{(k)}(s, a)$, $\forall (s, a) \in \mathcal{S} \times \mathcal{A}$
 - 6: Sample a n -step trajectory $(s_0^{(t)}, a_0^{(t)}, r_1^{(t)}, s_1^{(t)}, a_1^{(t)}, \dots, r_n^{(t)}, s_n^{(t)}, a_n^{(t)})$ from the MDP $\mathcal{M}^{(k)}$, according to ϵ -greedy policy derived from $Q_{\mathbf{w}^{(t)}}^{(k)}$
 - 7: Formulate $\mathbf{H}^{(t)}$ as in (4) with the sampled trajectory and current parameter $\mathbf{w}^{(t)}$
 - 8: Compute $\mathbf{w}^{(t+1)} = \text{TF}_{\theta^{(t)}}(\mathbf{H}^{(t)}) := \mathbf{w}^{(t)} + \frac{1}{n} [\mathbf{V}^{(t)} \mathbf{H}^{(t)} \mathbf{H}^{(t)\top} \mathbf{P}^{(t)} \mathbf{H}^{(t)}]_{-d:, -1}$
 - 9: Compute $\mathbf{w}_{\text{SARSA}}^{(t+1)}$ according to (2)
 - 10: Compute loss $\hat{L}^{(t)} = \frac{1}{2} \|\mathbf{w}^{(t+1)} - \mathbf{w}_{\text{SARSA}}^{(t+1)}\|^2$
 - 11: Update $\theta^{(t+1)} \leftarrow \theta^{(t)} - \eta \nabla_{\theta} \hat{L}^{(t)}$
 - 12: Update $s_0^{(t+1)} \leftarrow s_n^{(t)}$, $\mathbf{w}^{(t+1)} \leftarrow \mathbf{w}_{\text{SARSA}}^{(t+1)}$
 - 13: **end for**
 - 14: Update $\theta^{(0)} \leftarrow \theta^{(T)}$
 - 15: **end for**
 - 16: **Return** Trained transformer parameter θ
-

Proposition 3.1 (Invariant parameter groups). *Partition the attention parameters into four sub-blocks:*

$$\mathbf{P} = \begin{bmatrix} \mathbf{P}_{11} & \mathbf{P}_{12} \\ \mathbf{P}_{21} & \mathbf{P}_{22} \end{bmatrix}, \quad \mathbf{V} = \begin{bmatrix} \mathbf{V}_{11} & \mathbf{V}_{12} \\ \mathbf{V}_{21} & \mathbf{V}_{22} \end{bmatrix}, \quad (8)$$

where $\mathbf{P}_{11}, \mathbf{V}_{11} \in \mathbb{R}^{(2d+1) \times (2d+1)}$, $\mathbf{P}_{12}, \mathbf{V}_{12} \in \mathbb{R}^{(2d+1) \times (d+1)}$, $\mathbf{P}_{21}, \mathbf{V}_{21} \in \mathbb{R}^{(d+1) \times (2d+1)}$, and $\mathbf{P}_{22}, \mathbf{V}_{22} \in \mathbb{R}^{(d+1) \times (d+1)}$. Let $\bar{\mathbf{V}}_{21}$ and $\bar{\mathbf{V}}_{22}$ denote the last d rows of \mathbf{V}_{21} and \mathbf{V}_{22} , respectively. Under gradient flow (7), the following parameters are invariant:

- (i) The blocks $\mathbf{P}_{11}, \mathbf{P}_{21}, \mathbf{V}_{11}, \mathbf{V}_{12}$ and the first rows of $\mathbf{V}_{21}, \mathbf{V}_{22}$ do not affect the transformer output and remain unchanged throughout training.
- (ii) If $\mathbf{P}_{22}^{(0)} = \mathbf{0}$ and $\bar{\mathbf{V}}_{22}^{(0)} = \mathbf{0}$, then $\mathbf{P}_{22}^{(t)} = \mathbf{0}$ and $\bar{\mathbf{V}}_{22}^{(t)} = \mathbf{0}$ for all $t \geq 0$.

The proof is deferred to Appendix F. Throughout the remainder of this section, we restrict our analysis to initializations satisfying $\mathbf{P}_{22}^{(0)} = \mathbf{0}$ and $\bar{\mathbf{V}}_{22}^{(0)} = \mathbf{0}$. By Proposition 3.1(ii), this constraint is preserved by gradient flow, and combined with (i) it reduces the training dynamics on (\mathbf{P}, \mathbf{V}) to dynamics on the effective parameter $\theta_{\text{eff}} := (\mathbf{P}_{12}, \bar{\mathbf{V}}_{21}) \in \Theta_{\text{eff}}$, where $\Theta_{\text{eff}} = \mathbb{R}^{(2d+1) \times (d+1)} \times \mathbb{R}^{d \times (2d+1)}$ is the effective parameter space. From (5), the optimum structures of these sub-blocks are

$$\mathbf{P}_{12}^* := \begin{bmatrix} \mathbf{0}_{d \times 1} & -\mathbf{I}_d \\ \mathbf{0}_{d \times 1} & \mathbf{I}_d \\ 1 & \mathbf{0}_{1 \times d} \end{bmatrix} \in \mathbb{R}^{(2d+1) \times (d+1)}, \quad \bar{\mathbf{V}}_{21}^* := [\alpha \mathbf{I}_d \quad \mathbf{0}_{d \times d} \quad \mathbf{0}_{d \times 1}] \in \mathbb{R}^{d \times (2d+1)},$$

subject to the scaling freedom $(\mathbf{P}_{12}^*, \bar{\mathbf{V}}_{21}^*) \mapsto (c\mathbf{P}_{12}^*, c^{-1}\bar{\mathbf{V}}_{21}^*)$ for any $c \neq 0$. Without loss of generality we restrict to $c > 0$ (the sign-flipped branch is handled by symmetry), and to a compact sub-interval $I = [c_-, c_+] \subset (0, \infty)$ bounded away from the degenerate limits $c \rightarrow 0, \infty$. On this interval, we define the *optimal parameter manifold*

$$\mathfrak{M}_I := \{\bar{\theta}_{\text{eff}}(c) := (c\mathbf{P}_{12}^*, c^{-1}\bar{\mathbf{V}}_{21}^*) : c \in I\} \subset \Theta_{\text{eff}}, \quad (9)$$

and the normal space at $\bar{\theta}_{\text{eff}}(c)$ as

$$N_c \mathfrak{M}_I := \{(\mathbf{U}, \mathbf{W}) \in \Theta_{\text{eff}} : \langle \mathbf{U}, \mathbf{P}_{12}^* \rangle_F - c^{-2} \langle \mathbf{W}, \bar{\mathbf{V}}_{21}^* \rangle_F = 0\}.$$

We now state the richness assumptions on the training-MDP distribution that ensure local convergence to the optimal parameter manifold (9).

Assumption 1 (Richness of training MDPs). Let Π denote the class of behavior policies used to generate training trajectories. There exist positive constants $B_\phi, B_r, B_{\tilde{w}}, \kappa_{\tilde{w}}, \kappa_R, \kappa_q$ and $\rho \in [0, 1]$ such that, for every $\pi \in \Pi$:

- (1) **Boundedness.** Almost surely, $\|\phi(s, a)\| \leq B_\phi$, $|r| \leq B_r$, and $\|\tilde{\mathbf{w}}\| \leq B_{\tilde{w}}$.
- (2) **Parameter excitation.** $\mathbb{E}[\tilde{\mathbf{w}}\tilde{\mathbf{w}}^\top] \succeq \kappa_{\tilde{w}}\mathbf{I}_{d+1}$.
- (3) **Bellman-regressor excitation.** $\mathbb{E}[\mathbf{R}(z)^\top \mathbf{R}(z) \mid \mathbf{w}] \succeq \kappa_R \mathbf{I}_{2d+1}$ for every $\mathbf{w} \in \mathbb{R}^d$.
- (4) **TD-target excitation.** $\mathbb{E}[\mathbf{b}(z)\mathbf{b}(z)^\top] \succeq \kappa_q \mathbf{I}_{2d+1}$.
- (5) **No destructive cancellation.** For every $c \in I$ and $(\mathbf{U}, \mathbf{W}) \in N_c \mathfrak{M}_I$,

$$\left| \mathbb{E}_z \langle \mathbf{R}(z) \mathbf{U} \tilde{\mathbf{w}}, \mathbf{W} \mathbf{b}(z) \rangle \right| \leq \rho \sqrt{\mathbb{E}_z \|\mathbf{R}(z) \mathbf{U} \tilde{\mathbf{w}}\|^2 \cdot \mathbb{E}_z \|\mathbf{W} \mathbf{b}(z)\|^2}.$$

We emphasize that Assumptions (1)–(2) can be enforced by construction: normalize features and clip rewards to achieve boundedness, and sample \mathbf{w} from an isotropic distribution to ensure parameter excitation. Assumptions (3)–(5) are structural conditions on the trajectory distribution that are satisfied generically: under a random feature map ϕ , random rewards, and ϵ -greedy exploration ($\epsilon > 0$), the trajectory distribution provides excitation in the \mathbf{R} and \mathbf{b} directions, and the cross-correlation bound $\rho < 1$ holds in typical non-degenerate cases. Verification for specific MDP families is deferred to future work.

Theorem 3.2 (Local convergence to the optimal parameter manifold). *Under Assumption 1, let*

$$B_\Sigma := 2B_\phi^2 + B_r^2, \quad C_Q := \frac{1}{2} B_\Sigma B_{\tilde{w}},$$

$$m_0 := (1 - \rho) \min \{ c_+^{-2} \alpha^2 \kappa_R \kappa_{\tilde{w}}, c_-^2 \kappa_q \}, \quad M_0 := B_\Sigma^2 B_{\tilde{w}}^2 (c_-^{-2} \alpha^2 + 2c_+^2).$$

Define the tube

$$\mathcal{T}_r(I) := \{ \bar{\boldsymbol{\theta}}_{\text{eff}}(c) + \Delta : c \in I, \Delta \in N_c \mathfrak{M}_I, \|\Delta\| < r \}, \quad (10)$$

where $0 < r < \frac{\sqrt{m_0}}{3C_Q}$. Fix a compact subinterval $I_0 \subset \text{int}(I)$. Let

$$\eta_{I_0, r} := \text{dist}(\mathfrak{M}_{I_0}, \boldsymbol{\Theta}_{\text{eff}} \setminus \mathcal{T}_r(I)), \quad (11)$$

Suppose the initial parameter $\boldsymbol{\theta}_{\text{eff}}(0)$ satisfies the following condition:

$$\text{dist}(\boldsymbol{\theta}_{\text{eff}}(0), \mathfrak{M}_{I_0}) < \min \left(r, \frac{\eta_{I_0, r}}{1 + \frac{K_r(\sqrt{M_0} + C_Q r)}{\sqrt{2\mu_r}}} \right), \quad (12)$$

where $K_r := \sqrt{2} B_\Sigma B_{\tilde{w}} \left((c_+ \sqrt{2d+1} + r)^2 + (c_-^{-1} \sqrt{d} + r)^2 \right)^{1/2}$. Consider the gradient flow (7) with initial point $\boldsymbol{\theta}_{\text{eff}}(0)$. Then the gradient flow solution exists for all $t \geq 0$, remains in $\mathcal{T}_r(I)$, and satisfies

$$\mathcal{L}(\boldsymbol{\theta}_{\text{eff}}(t)) \leq e^{-2\mu_r t} (\mathcal{L}(\boldsymbol{\theta}_{\text{eff}}(0))),$$

where $\mu_r := \frac{(m_0 - 3C_Q \sqrt{m_0} r)^2}{(\sqrt{M_0} + C_Q r)^2}$. Furthermore, $\boldsymbol{\theta}_{\text{eff}}(t)$ converges to a point $\boldsymbol{\theta}_{\text{eff}}(\infty) \in \mathfrak{M}_I$, and

$$\|\boldsymbol{\theta}_{\text{eff}}(t) - \boldsymbol{\theta}_{\text{eff}}(\infty)\| \leq \frac{K_r}{\mu_r} \sqrt{\mathcal{L}(\boldsymbol{\theta}_{\text{eff}}(0))} e^{-\mu_r t}.$$

Theorem 3.2 establishes that, when initialized sufficiently close to the optimal manifold \mathfrak{M}_I , gradient flow provably converges to a point on that manifold at an exponential rate governed by μ_r . The key insight is that under Assumption 1 on the training MDPs, the loss function exhibits local contractivity: the manifold itself is a level set, but perturbations perpendicular to it decay exponentially. To briefly summarize our proof strategy, we first define the tube (10), which specifies the region around \mathfrak{M}_I where a local Polyak–Łojasiewicz (PL) inequality holds (Lemma C.2). Next, the buffer distance (11) quantifies the slackness between the inner manifold patch \mathfrak{M}_{I_0} and the boundary of the tube, providing the margin a trajectory can travel before risking exit. The initialization condition (12) then bounds the cumulative gradient-flow displacement by this margin $\eta_{I_0, r}$, which ensures that the trajectory never leaves the tube and the PL inequality remains active for all $t \geq 0$. The complete proof is deferred to Appendix G.

3.3 Transformers can implement Actor-Critic

Having established both existence and convergence for the SARSA-based ICRL implementation, we now ask whether an analogous construction extends to the actor-critic method (3), in which the transformer must jointly update a value function and a parameterized policy. To accommodate this, we construct the input prompt as follows:

$$\mathbf{H} = \begin{bmatrix} \phi_V(s_0) & \cdots & \phi_V(s_{n-1}) & \mathbf{0} \\ \gamma\phi_V(s_1) & \cdots & \gamma\phi_V(s_n) & \mathbf{0} \\ r_1 & \cdots & r_n & 0 \\ \gamma^0 \mathbf{g}_\lambda(s_0, a_0) & \cdots & \gamma^{n-1} \mathbf{g}_\lambda(s_{n-1}, a_{n-1}) & \mathbf{0} \\ 0 & \cdots & 0 & 1 \\ \mathbf{0} & \cdots & \mathbf{0} & \boldsymbol{\lambda} \\ \mathbf{0} & \cdots & \mathbf{0} & \mathbf{w} \end{bmatrix} \in \mathbb{R}^{D \times (n+1)}, \quad (13)$$

where $D = 3d + 2m + 2$. Compared to the SARSA prompt (4), the construction in (13) additionally encodes the discounted score function terms $\gamma^i \mathbf{g}_\lambda(s_i, a_i)$ and the current actor parameter $\boldsymbol{\lambda}$. The following theorem shows that a single transformer block can still exactly implement the batch actor-critic update.

Theorem 3.3 (Implementing Actor-Critic with a transformer block). *Let the output projection function be $f_{\text{read}}(\cdot) = \cdot_{-(d+m):, -1}$, which extracts the last $(d+m)$ entries of the final column. Given the input prompt (13), for any $\alpha, \beta > 0$ there exist parameters $\boldsymbol{\theta}^* = \{c\mathbf{P}^*, c^{-1}\mathbf{V}^*\} \subseteq \mathbb{R}^{D \times D}$ with $c \neq 0$ and*

$$\mathbf{P}^* = \begin{bmatrix} *_{(2d+m+1) \times (2d+m+1)} & \begin{bmatrix} \mathbf{0}_{d \times 1} & \mathbf{0}_{d \times m} & -\mathbf{I}_{d \times d} \\ \mathbf{0}_{d \times 1} & \mathbf{0}_{d \times m} & \mathbf{I}_{d \times d} \\ 1 & \mathbf{0}_{1 \times m} & \mathbf{0}_{1 \times d} \\ \mathbf{0}_{m \times 1} & \mathbf{0}_{m \times m} & \mathbf{0}_{m \times d} \end{bmatrix} \\ *_{(d+m+1) \times (2d+m+1)} & \mathbf{0}_{(d+m+1) \times (d+m+1)} \end{bmatrix}, \quad (14)$$

$$\mathbf{V}^* = \begin{bmatrix} *_{(2d+m+1) \times (2d+m+1)} & *_{(2d+m+1) \times (d+m+1)} \\ \begin{bmatrix} *_{1 \times d} & *_{1 \times d} & *_{1 \times 1} & *_{1 \times m} \\ \mathbf{0}_{m \times d} & \mathbf{0}_{m \times d} & \mathbf{0}_{m \times 1} & \alpha \mathbf{I}_{m \times m} \\ \beta \mathbf{I}_{d \times d} & \mathbf{0}_{d \times d} & \mathbf{0}_{d \times 1} & \mathbf{0}_{d \times m} \end{bmatrix} & \begin{bmatrix} *_{1 \times (d+m+1)} \\ \mathbf{0}_{m \times (d+m+1)} \\ \mathbf{0}_{d \times (d+m+1)} \end{bmatrix} \end{bmatrix},$$

such that the transformer $TF_{\boldsymbol{\theta}^*}$ directly implements the batch actor-critic update (3).

The proof of Theorem 3.3 is provided in Appendix H. Similar to SARSA, we design a training procedure to learn the transformer parameters $\boldsymbol{\theta}$ in Algorithm 2 in Appendix B. The convergence analysis follows the analogous arguments as in the SARSA setting and is therefore omitted. Empirical validation of convergence is provided in Section 4.

4 Experiments

We empirically demonstrate that gradient-based training of a single linear self-attention block converges to the optimal parameter manifold characterized in Theorem 3.1 and Theorem 3.3, using Algorithm 1 and Algorithm 2 respectively. Furthermore, we evaluate the control performance of the trained transformers, showing their ability to perform policy improvement on unseen MDPs. Additional details and experiments can be found in Appendix I.

4.1 Training

Common Training Setup. Both experiments share the same training MDP family. Each MDP has $n_S = 9$ states and $n_A = 4$ actions, with discount $\gamma = 0.5$. For each MDP, the initial-state distribution P_0 and transition kernel $P(\cdot | s, a)$ are drawn independently from Dirichlet(1, ..., 1) (uniform over the probability simplex on n_S states), and the rewards $r(a, s') \sim \text{Unif}(-1, 1)$ are sampled i.i.d. per (a, s') . Trajectories of window length $n = 20$ are rolled out with horizon $T = 1000$. In both experiments, the in-context learner is a one-layer transformer with corresponding embedding dimension D . Following Proposition 3.1, the inert blocks $\mathbf{P}_{11}, \mathbf{P}_{21}, \mathbf{V}_{11}, \mathbf{V}_{12}, \mathbf{P}_{22}, \mathbf{V}_{22}$ are initialized to zero, while the effective sub-blocks ($\mathbf{P}_{12}, \bar{\mathbf{V}}_{21}$) are initialized with Xavier-normal

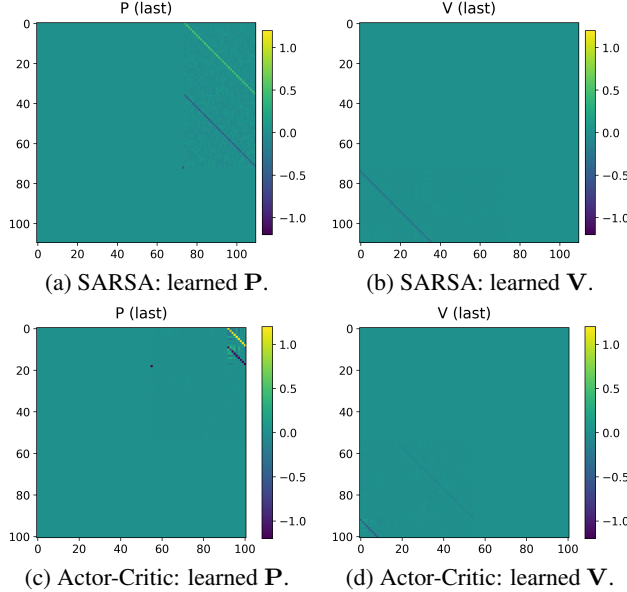


Figure 2: Final learned \mathbf{P} and \mathbf{V} matrices after training, for the SARSA transformer (top row) and the Actor-Critic transformer (bottom row). In both settings, the non-zero structure matches the theoretical constructions (\mathbf{P}^* , \mathbf{V}^*) in (5) and (14).

entries (gain 0.1). Training is performed over $K = 10,000$ independently sampled MDPs using Adam optimizer [Kingma and Ba, 2015] with initial learning rate $\eta = 10^{-3}$ and exponential decay by a factor of 0.99 every 10 MDPs.

SARSA experiment specifications. For each MDP, the state–action feature map $\phi : \mathcal{S} \times \mathcal{A} \rightarrow \mathbb{R}^d$ ($d = n_{\mathcal{S}}n_{\mathcal{A}} = 36$) and the initial weight $\mathbf{w}^{(0)} \in \mathbb{R}^d$ have entries drawn i.i.d. from $\text{Unif}(-1, 1)$. The behavior policy is ϵ -greedy ($\epsilon = 0.1$) with $Q(s, a) = \phi(s, a)^\top \mathbf{w}$, and the SARSA target $\mathbf{w}_{\text{SARSA}}$ is computed from the trajectory window with step size $\alpha = 0.2$. The transformer uses embedding dimension $D = 3d + 2 = 110$.

Actor-Critic experiment specifications. For each MDP, the policy feature $\phi_\pi : \mathcal{S} \times \mathcal{A} \rightarrow \mathbb{R}^m$ ($m = 36$), value feature $\phi_V : \mathcal{S} \rightarrow \mathbb{R}^d$ ($d = 9$), and initial weights $\lambda^{(0)} \in \mathbb{R}^m$, $\mathbf{w}^{(0)} \in \mathbb{R}^d$ are drawn i.i.d. from $\text{Unif}(-1, 1)$. The behavior policy follows $\pi(a | s) \propto \exp(\phi_\pi(s, a)^\top \lambda)$, with $\epsilon = 0.1$ – random exploration. At each step, the teacher applies a one-step critic update to \mathbf{w} (step size $\beta = 0.8$) and an actor update to λ (step size $\alpha = 0.2$). The transformer uses embedding dimension $D = 3d + 2m + 2 = 101$.

Results. In both experiments, the training loss decays approximately exponentially to zero (see Appendix I.1). Figure 2 shows the learned \mathbf{P} and \mathbf{V} matrices: the upper-right block of \mathbf{P} and the relevant rows of the lower-left block of \mathbf{V} recover the structure of (\mathbf{P}^* , \mathbf{V}^*) in (5) and (14) (up to scaling), while other blocks remain near zero. This confirms that the ICRL training algorithms 1 and 2 drive the parameters toward the optimal manifold.

4.2 Evaluation

Beyond parameter-level fidelity, we evaluate whether the trained transformer, when deployed as an in-context update rule on unseen MDPs, induces high-return policies. We randomly sample $K = 100$ test MDPs with corresponding features, disjoint from the training set. For each MDP, we run closed-loop in-context updates: at each step, the prompt $\mathbf{H}^{(t)}$ is fed to the transformer to produce $\mathbf{w}^{(t+1)}$ (or $(\lambda^{(t+1)}, \mathbf{w}^{(t+1)})$ in the actor–critic setting), which defines the behavior policy used to generate the next trajectory window. Every 10 update steps, we freeze the iterate and estimate the discounted return via Monte Carlo using 32 trajectories of length 50, with initial state $s_0 \sim P_0^{(k)}$.

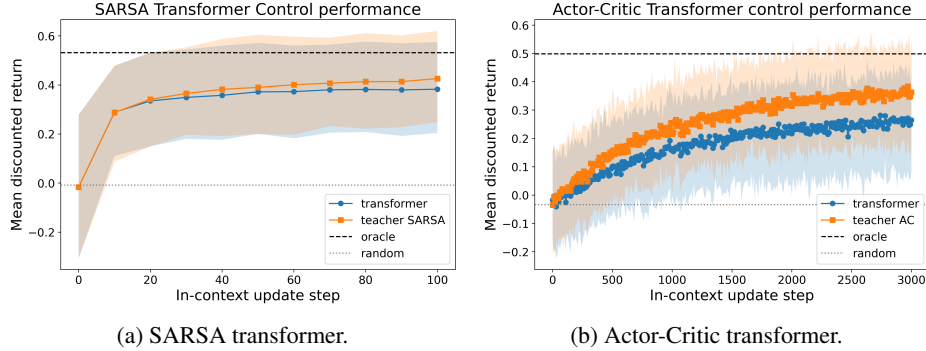


Figure 3: Closed-loop control performance on 100 held-out random MDPs versus in-context update step t . Curves show the per-MDP return averaged across MDPs (shaded: 25–75% interquartile band). The transformer curve closely tracks the teacher curve in both settings, indicating that the trained model approximately implements the analytical update rule at deployment.

We compare against analytical teacher updates (SARSA (2) and actor–critic (3)) executed in the same closed loop, the oracle greedy policy under Q^* obtained by exact value iteration on $(P^{(k)}, R^{(k)})$, and a uniform random policy. Figure 3 reports the average return across MDPs. In both settings, the transformer closely tracks the teacher: performance improves rapidly from near-random initialization and approaches the oracle as t increases. Crucially, this consistency persists across long in-context horizons, indicating that the transformer faithfully implements the teacher update rule rather than merely mimicking short-horizon behavior.

Notably, the remaining gap to the oracle reflects limitations of the linear function approximation rather than imperfect imitation, since the same gap is also observed for the analytical teacher. These results show that convergence to the optimal parameter manifold (Theorem 3.2) translates into strong policy-level performance, with the trained transformer accurately reproducing the analytical update rules at deployment.

5 Conclusion

In this work, we demonstrate that transformers can provably implement ICRL algorithms that perform policy improvement. Through explicit constructions, we show that a single linear-attention block can realize batch SARSA and actor-critic updates. Furthermore, we provide the first convergence guarantee in the ICRL literature, proving that under suitable richness conditions on the training MDPs, gradient-flow training to mimic the teacher update converges locally to the optimal parameter manifold. Our empirical results validate these theoretical findings, showing that trained transformers recover the predicted parameter structures and achieve strong control performance on unseen MDPs. These results help bridge the gap between the theoretical understanding and practical implementation of ICRL, suggesting that the transformer architecture naturally favors learning and implementing reinforcement-learning algorithmic structures. Overall, this work advances our understanding of how transformers perform RL algorithms in context, with implications for both AI safety and the design of more capable learning systems.

5.1 Limitations

Our work has several limitations that need to be addressed in future work. First, Assumption 1 imposes richness conditions on the training MDPs that may be difficult to verify in practice. While such conditions are expected to hold generically under random features, rewards, and sufficient exploration, precisely characterizing the required trajectory diversity remains open. Second, our convergence guarantee is local and requires initialization near the optimal manifold; understanding the global optimization landscape is an important direction for future work. Finally, our analysis focuses on deterministic gradient flow in a simplified setting, leaving extensions to stochastic optimization and more complex transformer architectures for future study.

References

- Tom Brown, Benjamin Mann, Nick Ryder, Melanie Subbiah, Jared D Kaplan, Prafulla Dhariwal, Arvind Neelakantan, Pranav Shyam, Girish Sastry, Amanda Askell, Sandhini Agarwal, Ariel Herbert-Voss, Gretchen Krueger, Tom Henighan, Rewon Child, Aditya Ramesh, Daniel Ziegler, Jeffrey Wu, Clemens Winter, Chris Hesse, Mark Chen, Eric Sigler, Mateusz Litwin, Scott Gray, Benjamin Chess, Jack Clark, Christopher Berner, Sam McCandlish, Alec Radford, Ilya Sutskever, and Dario Amodei. Language models are few-shot learners. In *Proceedings of Neural Information Processing Systems*, Virtual, December 2020. URL <https://arxiv.org/abs/2005.14165>.
- Shivam Garg, Dimitris Tsipras, Percy S Liang, and Gregory Valiant. What can transformers learn in-context? a case study of simple function classes. In *Proceedings of Neural Information Processing Systems*, New Orleans, LA, USA, December 2022. URL <https://arxiv.org/abs/2208.01066>.
- Qingxiu Dong, Lei Li, Damai Dai, Ce Zheng, Jingyuan Ma, Rui Li, Heming Xia, Jingjing Xu, Zhiyong Wu, Tianyu Liu, Baobao Chang, Xu Sun, Lei Li, and Zhifang Sui. A survey on in-context learning, 2024. URL <https://arxiv.org/abs/2301.00234>.
- Ashish Vaswani, Noam Shazeer, Niki Parmar, Jakob Uszkoreit, Llion Jones, Aidan N Gomez, Lukasz Kaiser, and Illia Polosukhin. Attention is all you need. In *Proceedings of Neural Information Processing Systems*, Long Beach, CA, USA, December 2017. URL https://proceedings.neurips.cc/paper_files/paper/2017/file/3f5ee243547dee91fbd053c1c4a845aa-Paper.pdf.
- Aakanksha Chowdhery, Sharan Narang, Jacob Devlin, Maarten Bosma, Gaurav Mishra, Adam Roberts, Paul Barham, Hyung Won Chung, Charles Sutton, Sebastian Gehrmann, et al. PaLM: Scaling language modeling with pathways. *Journal of Machine Learning Research*, 24(240):1–113, 2023.
- OpenAI, Josh Achiam, Steven Adler, Sandhini Agarwal, Lama Ahmad, Ilge Akkaya, Florencia Leoni Aleman, Diogo Almeida, Janko Altenschmidt, Sam Altman, Shyamal Anadkat, et al. GPT-4 technical report. *arXiv preprint arXiv:2303.08774*, 2024. URL <https://arxiv.org/abs/2303.08774>.
- Johannes von Oswald, Eyvind Niklasson, Ettore Randazzo, João Sacramento, Alexander Mordvintsev, Andrey Zhmoginov, and Max Vladymyrov. Transformers learn in-context by gradient descent. In *Proceedings of the 40th International Conference on Machine Learning*, 2023. URL <https://arxiv.org/abs/2212.07677>.
- Ekin Akyürek, Dale Schuurmans, Jacob Andreas, Tengyu Ma, and Denny Zhou. What learning algorithm is in-context learning? Investigations with linear models. In *The Eleventh International Conference on Learning Representations*, 2023. URL <https://openreview.net/forum?id=0gOX4H8yN4I>.
- Kwangjun Ahn, Xiang Cheng, Hadi Daneshmand, and Suvrit Sra. Transformers learn to implement preconditioned gradient descent for in-context learning. In *Thirty-seventh Conference on Neural Information Processing Systems*, 2023. URL <https://openreview.net/forum?id=LziniAXEI9>.
- Arvind Mahankali, Tatsunori B. Hashimoto, and Tengyu Ma. One step of gradient descent is provably the optimal in-context learner with one layer of linear self-attention. In *The Twelfth International Conference on Learning Representations*, 2024. URL <https://arxiv.org/abs/2307.03576>.
- Yu Bai, Fan Chen, Huan Wang, Caiming Xiong, and Song Mei. Transformers as statisticians: Provable in-context learning with in-context algorithm selection. In *Thirty-seventh Conference on Neural Information Processing Systems*, 2023. URL <https://openreview.net/forum?id=1iMSqUuVg9>.
- Ruiqi Zhang, Spencer Frei, and Peter L. Bartlett. Trained transformers learn linear models in-context. In *Journal of Machine Learning Research*, 2024. URL <https://arxiv.org/abs/2306.09927>.

- Haodong Liang, Krishna Balasubramanian, and Lifeng Lai. Transformers handle endogeneity in in-context linear regression. In *The Thirteenth International Conference on Learning Representations*, 2025. URL <https://openreview.net/forum?id=QfhU3ZC2g1>.
- Michael Laskin, Luyu Wang, Junhyuk Oh, Emilio Parisotto, Stephen Spencer, Richie Steigerwald, DJ Strouse, Steven Stenberg Hansen, Angelos Filos, Ethan Brooks, Maxime Gazeau, Himanshu Sahni, Satinder Singh, and Volodymyr Mnih. In-context reinforcement learning with algorithm distillation. In *The Eleventh International Conference on Learning Representations*, 2023. URL <https://openreview.net/forum?id=hy0a5MMPUv>.
- Licong Lin, Yu Bai, and Song Mei. Transformers as decision makers: Provable in-context reinforcement learning via supervised pretraining. In *The Twelfth International Conference on Learning Representations*, 2024. URL <https://arxiv.org/abs/2310.08566>.
- Amir Moeini, Jiuqi Wang, Jacob Beck, Ethan Blaser, Shimon Whiteson, Rohan Chandra, and Shangtong Zhang. A survey of in-context reinforcement learning, 2025. URL <https://arxiv.org/abs/2502.07978>.
- Richard S. Sutton and Andrew G. Barto. *Reinforcement Learning: An Introduction*. MIT Press, Cambridge, MA, 2 edition, 2018.
- Jonathan Lee, Annie Xie, Aldo Pacchiano, Yash Chandak, Chelsea Finn, Ofir Nachum, and Emma Brunskill. Supervised pretraining can learn in-context reinforcement learning. In *Thirty-seventh Conference on Neural Information Processing Systems*, 2023. URL <https://openreview.net/forum?id=dCYBAGQXLo>.
- Ethan Brooks, Logan Walls, Richard L. Lewis, and Satinder Singh. Large language models can implement policy iteration. In *Thirty-seventh Conference on Neural Information Processing Systems*, 2023. URL <https://arxiv.org/abs/2210.03821>.
- Sharath Chandra Raparthi, Eric Hambro, Robert Kirk, Mikael Henaff, and Roberta Raileanu. Learning to solve new sequential decision-making tasks with in-context learning. In *NeurIPS 2023 Foundation Models for Decision Making Workshop*, 2023. URL <https://openreview.net/forum?id=JB3H6LS1PY>.
- Jiuqi Wang, Ethan Blaser, Hadi Daneshmand, and Shangtong Zhang. Transformers can learn temporal difference methods for in-context reinforcement learning. In *The Thirteenth International Conference on Learning Representations*, 2025. URL <https://openreview.net/forum?id=Pj06mxCXPl>.
- Diederik P. Kingma and Jimmy Ba. Adam: A method for stochastic optimization. In *International Conference on Learning Representations (ICLR)*, 2015. URL <https://arxiv.org/abs/1412.6980>.
- Lili Chen, Kevin Lu, Aravind Rajeswaran, Kimin Lee, Aditya Grover, Michael Laskin, Pieter Abbeel, Aravind Srinivas, and Igor Mordatch. Decision transformer: Reinforcement learning via sequence modeling. In A. Beygelzimer, Y. Dauphin, P. Liang, and J. Wortman Vaughan, editors, *Advances in Neural Information Processing Systems*, 2021. URL <https://openreview.net/forum?id=a7APmM4B9d>.
- Michael Janner, Qiyang Li, and Sergey Levine. Offline reinforcement learning as one big sequence modeling problem. In M. Ranzato, A. Beygelzimer, Y. Dauphin, P.S. Liang, and J. Wortman Vaughan, editors, *Advances in Neural Information Processing Systems*, volume 34, pages 1273–1286. Curran Associates, Inc., 2021. URL https://proceedings.neurips.cc/paper_files/paper/2021/file/099fe6b0b444c23836c4a5d07346082b-Paper.pdf.
- Jake Grigsby, Linxi Fan, and Yuke Zhu. AMAGO: Scalable in-context reinforcement learning for adaptive agents. In *The Twelfth International Conference on Learning Representations*, 2024. URL <https://openreview.net/forum?id=M6XWoEdmwf>.
- Akshay Krishnamurthy, Keegan Harris, Dylan J Foster, Cyril Zhang, and Aleksandrs Slivkins. Can large language models explore in-context? In *The Thirty-eighth Annual Conference on Neural Information Processing Systems*, 2024. URL <https://openreview.net/forum?id=OWPzhVqIux>.

- Yu Huang, Yuan Cheng, and Yingbin Liang. In-context convergence of transformers, 2023. URL <https://arxiv.org/abs/2310.05249>.
- Siyu Chen, Heejune Sheen, Tianhao Wang, and Zhuoran Yang. Training dynamics of multi-head softmax attention in in-context learning: Emergence, convergence, and optimality, 2024. URL <https://arxiv.org/abs/2402.19442>.
- Yuangdong Tian, Yiping Wang, Beidi Chen, and Simon Du. Scan and snap: Understanding training dynamics and token composition in 1-layer transformer. In *Thirty-seventh Conference on Neural Information Processing Systems*, 2023. URL <https://arxiv.org/abs/2305.16380>.
- Eshaan Nichani, Alex Damian, and Jason D. Lee. How transformers learn causal structure with gradient descent. In *Forty-first International Conference on Machine Learning*, 2024. URL <https://openreview.net/forum?id=jNM4imlHZv>.

A Additional Related Works

In this appendix, we discuss additional works that are related to our paper.

In-context learning theory for supervised tasks. Garg et al. [2022] initiate this discussion on simple function classes, showing empirically that a transformer trained from scratch can in-context learn linear regression, two-layer neural networks, and decision trees. A subsequent line of mechanistic work then asks *how* such behavior arises. von Oswald et al. [2023] and Akyürek et al. [2023] argue that transformers implement gradient descent or closed-form least squares on the in-context examples, and Ahn et al. [2023] and Mahankali et al. [2024] prove that, on linear regression, the optimal one-layer linear self-attention block is exactly one step of preconditioned gradient descent. Bai et al. [2023] broaden the picture by showing that transformers can implement a wide family of statistical estimators – including ridge regression, Lasso, and gradient descent on generalized linear models – and can even perform algorithm selection in context. Liang et al. [2025] further extend this line to in-context linear regression with endogenous covariates, constructing a multi-layer transformer that implements two-stage least squares and showing that it consistently estimates the structural parameter under standard instrumental-variable assumptions.

In-context reinforcement learning. The view of RL as in-context sequence modeling was popularized by the Decision Transformer [Chen et al., 2021] and the Trajectory Transformer [Janner et al., 2021], which cast policy improvement as autoregressive prediction over offline trajectories. Building on this paradigm, Laskin et al. [2023] introduce *algorithm distillation*, in which a causal transformer trained on RL learning histories reproduces the underlying learning algorithm at inference time, and Lee et al. [2023] show that supervised pretraining over offline trajectories suffices to elicit ICRL on new tasks. Subsequent empirical work demonstrates that large language models can in-context execute policy iteration on tabular MDPs [Brooks et al., 2023]; that pretraining on sufficiently diverse trajectories enables transformers to generalize to unseen sequential decision-making tasks purely from their context [Raparthy et al., 2023]; that scalable long-context architectures such as AMAGO learn adaptive policies in context across challenging environments [Grigsby et al., 2024]; and that LLMs can perform nontrivial exploration in bandit and small MDP problems even without external scaffolding [Krishnamurthy et al., 2024]. On the theoretical side, Lin et al. [2024] prove that supervised pretraining of transformers on offline trajectories yields near-optimal posterior-sampling policies, establishing sample-complexity guarantees for ICRL pretraining. The work most closely related to ours is Wang et al. [2025], which shows that a linear-attention block admits an invariant set under the expected gradient update of a value-prediction loss, thereby implementing policy evaluation via TD methods. Our work extends this line in two directions: from policy evaluation to policy improvement (SARSA and actor-critic), and from invariance to convergence of gradient training.

Training Dynamics. A complementary line of work studies the optimization landscape and training dynamics of attention itself, asking whether the in-context algorithms identified by mechanistic constructions are actually recoverable by gradient-based learning. Zhang et al. [2024] prove that gradient flow on a single linear self-attention block trained on random linear-regression tasks converges to the global minimum and recovers the preconditioned-gradient-descent solution predicted by Ahn et al. [2023], Mahankali et al. [2024]. Huang et al. [2023] extend such convergence guarantees to softmax

attention under orthogonal feature assumptions, and Chen et al. [2024] analyze multi-head softmax attention in the in-context regression setting, identifying an emergent task-specialization phenomenon en route to the global minimizer. From a different angle, Tian et al. [2023] dissect token-level dynamics of one-layer attention during language pretraining, while Nichani et al. [2024] show that transformers can recover hidden causal structure via gradient descent on synthetic tasks. These results are confined to supervised regression-style objectives. Our work pushes the training-dynamics analysis into ICRL, where the loss is non-convex and the optima form a one-dimensional scaling manifold rather than an isolated point.

B Training Algorithm

B.1 Actor-Critic Transformer

Algorithm 2 Actor Critic Transformer Training

- 1: **Input:** Transformer parameter $\theta^{(0)} = (\mathbf{P}^{(0)}, \mathbf{V}^{(0)})$, trajectory window length n , number of frames per MDP T , number of MDPs K , ϵ -greedy parameter ϵ , learning rate η , actor step size α , and critic step size β
 - 2: **for** $k = 0, \dots, K - 1$ **do**
 - 3: Sample a MDP $\mathcal{M}^{(k)} = (\mathcal{S}, \mathcal{A}, P^{(k)}, R^{(k)}, \gamma)$, and generate corresponding feature map for policy $\phi_\pi^{(k)} : \mathcal{S} \times \mathcal{A} \rightarrow \mathbb{R}^m$, and feature map for state value function $\phi_V^{(k)} : \mathcal{S} \rightarrow \mathbb{R}^d$. Initialize parameters $\lambda^{(0)}$, $\mathbf{w}^{(0)}$, and state $s_0^{(0)}$ randomly
 - 4: **for** $t = 0, \dots, T - 1$ **do**
 - 5: Calculate policy $\pi_{\lambda^{(t)}}^{(k)}(a|s) = \frac{\exp\{\lambda^{(t)\top} \phi_\pi^{(k)}(s,a)\}}{\sum_b \exp\{\lambda^{(t)\top} \phi_\pi^{(k)}(s,b)\}}, \forall s \in \mathcal{S}, a \in \mathcal{A}$
 - 6: Estimate state value function $v_{\mathbf{w}^{(t)}}^{(k)}(s) = \mathbf{w}^{(t)\top} \phi_V^{(k)}(s), \forall s \in \mathcal{S}$
 - 7: Compute policy gradient $\mathbf{g}_{\lambda^{(t)}}^{(k)}(s, a) = \phi_\pi^{(k)}(s, a) - \sum_b \phi_\pi^{(k)}(s, b) \pi_{\lambda^{(t)}}^{(k)}(b|s), \forall (s, a) \in \mathcal{S} \times \mathcal{A}$
 - 8: Sample n steps $(s_0^{(t)}, a_0^{(t)}, r_1^{(t)}, s_1^{(t)}, a_1^{(t)}, \dots, r_n^{(t)}, s_n^{(t)}, a_n^{(t)})$ from the MDP $\mathcal{M}^{(k)}$, according to policy $\pi_{\lambda^{(t)}}^{(k)}$ with ϵ -greedy exploration
 - 9: Formulate $\mathbf{H}^{(t)}$ as in (13) with the sampled trajectory and current parameters $\lambda^{(t)}, \mathbf{w}^{(t)}$
 - 10: Compute $\begin{bmatrix} \lambda^{(t+1)} \\ \mathbf{w}^{(t+1)} \end{bmatrix} = \text{TF}_{\theta^{(t)}}(\mathbf{H}^{(t)}) := \begin{bmatrix} \lambda^{(t)} \\ \mathbf{w}^{(t)} \end{bmatrix} + \frac{1}{n} [\mathbf{V}^{(t)} \mathbf{H}^{(t)} \mathbf{H}^{(t)\top} \mathbf{P}^{(t)} \mathbf{H}^{(t)}]_{(d+m):, -1}$
 - 11: Compute $\mathbf{w}_{\text{AC}}^{(t+1)}$ and $\lambda_{\text{AC}}^{(t+1)}$ according to (3)
 - 12: Compute loss $\hat{L}^{(t)} = \frac{1}{2} \|\mathbf{w}^{(t+1)} - \mathbf{w}_{\text{AC}}^{(t+1)}\|^2 + \frac{1}{2} \|\lambda^{(t+1)} - \lambda_{\text{AC}}^{(t+1)}\|^2$
 - 13: Update $\theta^{(t+1)} \leftarrow \theta^{(t)} - \eta \nabla_{\theta} \hat{L}^{(t)}$
 - 14: Update $s_0^{(t+1)} \leftarrow s_n^{(t)}, \lambda^{(t+1)} \leftarrow \lambda_{\text{AC}}^{(t+1)}, \mathbf{w}^{(t+1)} \leftarrow \mathbf{w}_{\text{AC}}^{(t+1)}$
 - 15: **end for**
 - 16: Update $\theta^{(0)} \leftarrow \theta^{(T)}$
 - 17: **end for**
 - 18: **Return** Learned transformer parameter θ
-

Algorithm 2 extends Algorithm 1 to jointly learn both the value and policy parameters. At each iteration, trajectories are sampled from the MDP, and the corresponding actor-critic updates are computed as teacher signals for both the critic parameter \mathbf{w} and the actor parameter λ . The transformer parameters are then updated via gradient descent to match these targets. The empirical loss combines the squared errors for both parameter updates, encouraging the transformer to approximate the full actor-critic learning rule.

C Supporting Lemmas

Lemma C.1 (Transformer output decomposition). Consider a transformer block with parameters $\theta = \{(\mathbf{P}, \mathbf{V})\} \subseteq \mathbb{R}^{D \times D}$. We decompose the parameters into blocks as follows:

$$\mathbf{P} = \begin{bmatrix} \mathbf{P}_{11} & \mathbf{P}_{12} \\ \mathbf{P}_{21} & \mathbf{P}_{22} \end{bmatrix}, \quad \mathbf{V} = \begin{bmatrix} \mathbf{V}_{11} & \mathbf{V}_{12} \\ \mathbf{V}_{21} & \mathbf{V}_{22} \end{bmatrix},$$

where $\mathbf{P}_{11}, \mathbf{V}_{11} \in \mathbb{R}^{(2d+1) \times (2d+1)}$, $\mathbf{P}_{12}, \mathbf{V}_{12} \in \mathbb{R}^{(2d+1) \times (d+1)}$, $\mathbf{P}_{21}, \mathbf{V}_{21} \in \mathbb{R}^{(d+1) \times (2d+1)}$, and $\mathbf{P}_{22}, \mathbf{V}_{22} \in \mathbb{R}^{(d+1) \times (d+1)}$. Let the output projection function be $f_{\text{read}}(\cdot) = \cdot_{-d, -1}$, which extracts the last d elements of the last column. Denote $\tilde{\mathbf{w}} := [1 \quad \mathbf{w}]^\top$. Given formulated input prompt

$$\mathbf{H} = \begin{bmatrix} \mathbf{x}_0 & \cdots & \mathbf{x}_{n-1} & \mathbf{0} \\ \mathbf{0} & \cdots & \mathbf{0} & \tilde{\mathbf{w}} \end{bmatrix} \in \mathbb{R}^{D \times (n+1)},$$

the transformer output can then be written as:

$$\text{TF}_\theta(\mathbf{H}) = \mathbf{w} + \bar{\mathbf{V}}_{21} \hat{\Sigma} \mathbf{P}_{12} \tilde{\mathbf{w}} + \frac{1}{n} \bar{\mathbf{V}}_{22} \tilde{\mathbf{w}} \tilde{\mathbf{w}}^\top \mathbf{P}_{22} \tilde{\mathbf{w}}, \quad (15)$$

where $\hat{\Sigma} := \frac{1}{n} \sum_{i=0}^{n-1} \mathbf{x}_i \mathbf{x}_i^\top$, and $\bar{\mathbf{V}}_{21}, \bar{\mathbf{V}}_{22}$ denote the last d rows of \mathbf{V}_{21} and \mathbf{V}_{22} , respectively.

Lemma C.2 (Local Polyak–Łojasiewicz inequality). Suppose Assumption 1 holds, and let the optimal manifold \mathfrak{M}_I , the constants $B_{\tilde{\mathbf{w}}}, B_\Sigma, C_Q, m_0, M_0$, and the tube $\mathcal{T}_r(I)$ be as defined in Theorem 3.2. Then \mathcal{L} attains its minimum value $\mathcal{L}^* = 0$ on \mathfrak{M}_I , and for every $0 < r < \frac{\sqrt{m_0}}{3C_Q}$ the population loss satisfies

$$\frac{1}{2} \|\nabla \mathcal{L}(\theta_{\text{eff}})\|^2 \geq \mu_r (\mathcal{L}(\theta_{\text{eff}}) - \mathcal{L}^*), \quad \forall \theta_{\text{eff}} \in \mathcal{T}_r(I), \quad (16)$$

where

$$\mu_r := \frac{(m_0 - 3C_Q \sqrt{m_0} r)^2}{(\sqrt{M_0} + C_Q r)^2}.$$

D Proof of Supporting Lemmas

D.1 Proof of Lemma C.1

Proof. From (4), the input matrix is

$$\mathbf{H} = \begin{bmatrix} \mathbf{x}_0 & \cdots & \mathbf{x}_{n-1} & \mathbf{0} \\ \mathbf{0} & \cdots & \mathbf{0} & \tilde{\mathbf{w}} \end{bmatrix} \in \mathbb{R}^{D \times (n+1)}.$$

By the definition of the linear self-attention block in (1),

$$\mathbf{H}_{\text{out}} = \mathbf{H} + \frac{1}{n} (\mathbf{V}\mathbf{H})(\mathbf{H}^\top \mathbf{P}\mathbf{H}) \in \mathbb{R}^{D \times (n+1)},$$

and the readout extracts the last d entries of the last column of \mathbf{H}_{out} . Denote the last column of the input by

$$\mathbf{h}_{n+1} := \begin{bmatrix} \mathbf{0}_{2d+1} \\ \tilde{\mathbf{w}} \end{bmatrix} \in \mathbb{R}^D.$$

Then we have

$$\mathbf{H}_{\text{out}}[:, n+1] = \mathbf{h}_{n+1} + \frac{1}{n} (\mathbf{V}\mathbf{H})(\mathbf{H}^\top \mathbf{P}\mathbf{h}_{n+1}). \quad (17)$$

Using the block partition (8),

$$\mathbf{P}\mathbf{h}_{n+1} = \begin{bmatrix} \mathbf{P}_{11} & \mathbf{P}_{12} \\ \mathbf{P}_{21} & \mathbf{P}_{22} \end{bmatrix} \begin{bmatrix} \mathbf{0} \\ \tilde{\mathbf{w}} \end{bmatrix} = \begin{bmatrix} \mathbf{P}_{12} \tilde{\mathbf{w}} \\ \mathbf{P}_{22} \tilde{\mathbf{w}} \end{bmatrix}.$$

Hence

$$\begin{aligned} (\mathbf{H}^\top \mathbf{P} \mathbf{h}_{n+1})_{i+1} &= [\mathbf{x}_i^\top \quad \mathbf{0}] \begin{bmatrix} \mathbf{P}_{12} \tilde{\mathbf{w}} \\ \mathbf{P}_{22} \tilde{\mathbf{w}} \end{bmatrix} = \mathbf{x}_i^\top \mathbf{P}_{12} \tilde{\mathbf{w}}, \quad i = 0, \dots, n-1, \\ (\mathbf{H}^\top \mathbf{P} \mathbf{h}_{n+1})_{n+1} &= [\mathbf{0} \quad \tilde{\mathbf{w}}^\top] \begin{bmatrix} \mathbf{P}_{12} \tilde{\mathbf{w}} \\ \mathbf{P}_{22} \tilde{\mathbf{w}} \end{bmatrix} = \tilde{\mathbf{w}}^\top \mathbf{P}_{22} \tilde{\mathbf{w}}. \end{aligned} \quad (18)$$

Similarly,

$$\begin{aligned} (\mathbf{V} \mathbf{H})[:, i+1] &= \mathbf{V} \begin{bmatrix} \mathbf{x}_i \\ \mathbf{0} \end{bmatrix} = \begin{bmatrix} \mathbf{V}_{11} \mathbf{x}_i \\ \mathbf{V}_{21} \mathbf{x}_i \end{bmatrix}, \quad i = 0, \dots, n-1, \\ (\mathbf{V} \mathbf{H})[:, n+1] &= \mathbf{V} \begin{bmatrix} \mathbf{0} \\ \tilde{\mathbf{w}} \end{bmatrix} = \begin{bmatrix} \mathbf{V}_{12} \tilde{\mathbf{w}} \\ \mathbf{V}_{22} \tilde{\mathbf{w}} \end{bmatrix}. \end{aligned} \quad (19)$$

Expanding the matrix-vector product as a sum over columns and combining (18) and (19), we have

$$\begin{aligned} (\mathbf{V} \mathbf{H})(\mathbf{H}^\top \mathbf{P} \mathbf{h}_{n+1}) &= \sum_{i=0}^{n-1} \begin{bmatrix} \mathbf{V}_{11} \mathbf{x}_i \\ \mathbf{V}_{21} \mathbf{x}_i \end{bmatrix} \mathbf{x}_i^\top \mathbf{P}_{12} \tilde{\mathbf{w}} + \begin{bmatrix} \mathbf{V}_{12} \tilde{\mathbf{w}} \\ \mathbf{V}_{22} \tilde{\mathbf{w}} \end{bmatrix} \tilde{\mathbf{w}}^\top \mathbf{P}_{22} \tilde{\mathbf{w}} \\ &= \begin{bmatrix} \mathbf{V}_{11} (\sum_{i=0}^{n-1} \mathbf{x}_i \mathbf{x}_i^\top) \mathbf{P}_{12} \tilde{\mathbf{w}} + \mathbf{V}_{12} \tilde{\mathbf{w}} \tilde{\mathbf{w}}^\top \mathbf{P}_{22} \tilde{\mathbf{w}} \\ \mathbf{V}_{21} (\sum_{i=0}^{n-1} \mathbf{x}_i \mathbf{x}_i^\top) \mathbf{P}_{12} \tilde{\mathbf{w}} + \mathbf{V}_{22} \tilde{\mathbf{w}} \tilde{\mathbf{w}}^\top \mathbf{P}_{22} \tilde{\mathbf{w}} \end{bmatrix}. \end{aligned}$$

Thus, rescaling by $\frac{1}{n}$, the lower $(d+1)$ -dimensional block of (17) reads

$$\tilde{\mathbf{w}} + \mathbf{V}_{21} \hat{\Sigma} \mathbf{P}_{12} \tilde{\mathbf{w}} + \frac{1}{n} \mathbf{V}_{22} \tilde{\mathbf{w}} \tilde{\mathbf{w}}^\top \mathbf{P}_{22} \tilde{\mathbf{w}}.$$

Since $\tilde{\mathbf{w}} = [1, \mathbf{w}^\top]^\top$, the last d entries of $\tilde{\mathbf{w}}$ equal \mathbf{w} . The readout $f_{\text{read}}(\cdot) = \cdot_{-d, -1}$ extracts the last d rows of the lower block, which selects the last d rows of \mathbf{V}_{21} and \mathbf{V}_{22} , namely $\bar{\mathbf{V}}_{21}$ and $\bar{\mathbf{V}}_{22}$. Therefore,

$$\text{TF}_\theta(\mathbf{H}) = \mathbf{w} + \bar{\mathbf{V}}_{21} \hat{\Sigma} \mathbf{P}_{12} \tilde{\mathbf{w}} + \frac{1}{n} \bar{\mathbf{V}}_{22} \tilde{\mathbf{w}} \tilde{\mathbf{w}}^\top \mathbf{P}_{22} \tilde{\mathbf{w}},$$

which completes the proof. \square

D.2 Proof of Lemma C.2

Proof. For any effective parameter $\theta_{\text{eff}} = (\mathbf{P}_{12}, \bar{\mathbf{V}}_{21})$, define the auxiliary predictor

$$f_{\theta_{\text{eff}}}(z) := \bar{\mathbf{V}}_{21} \hat{\Sigma}(z) \mathbf{P}_{12} \tilde{\mathbf{w}} \in \mathbb{R}^d.$$

By Theorem 3.1, $(\mathbf{P}_{12}^*, \bar{\mathbf{V}}_{21}^*)$ is a global minimizer of \mathcal{L} with $\mathcal{L}^* = 0$, and the scaling identity $f_{(c\mathbf{P}_{12}^*, c^{-1}\bar{\mathbf{V}}_{21}^*)} = f_{(\mathbf{P}_{12}^*, \bar{\mathbf{V}}_{21}^*)}$ for every $c > 0$ implies that every point of \mathfrak{M}_I is a global minimizer. Consequently,

$$\mathcal{L}(\theta_{\text{eff}}) - \mathcal{L}^* = \frac{1}{2} \mathbb{E}_z \|f_{\theta_{\text{eff}}}(z) - f_{\bar{\theta}_{\text{eff}}(c)}(z)\|^2, \quad \forall c \in I. \quad (20)$$

Throughout the proof, we denote $\Delta = (\mathbf{U}, \mathbf{W}) \in N_c \mathfrak{M}_I$ with $\|\Delta\| \leq r$, where $\|\Delta\|^2 := \|\mathbf{U}\|_F^2 + \|\mathbf{W}\|_F^2$, and set $\theta_{\text{eff}} := \bar{\theta}_{\text{eff}}(c) + \Delta$. Write $\|\cdot\|_{L^2} := \sqrt{\mathbb{E}_z \|\cdot\|^2}$.

Step 1: Decomposition of the prediction error. By the definition of $f_{\theta_{\text{eff}}}$ together with $\theta_{\text{eff}} = (c\mathbf{P}_{12}^* + \mathbf{U}, c^{-1}\bar{\mathbf{V}}_{21}^* + \mathbf{W})$,

$$\begin{aligned} f_{\theta_{\text{eff}}}(z) &= (c^{-1}\bar{\mathbf{V}}_{21}^* + \mathbf{W}) \hat{\Sigma}(z) (c\mathbf{P}_{12}^* + \mathbf{U}) \tilde{\mathbf{w}}, \\ f_{\bar{\theta}_{\text{eff}}(c)}(z) &= c^{-1}\bar{\mathbf{V}}_{21}^* \hat{\Sigma}(z) c\mathbf{P}_{12}^* \tilde{\mathbf{w}} = \bar{\mathbf{V}}_{21}^* \hat{\Sigma}(z) \mathbf{P}_{12}^* \tilde{\mathbf{w}}. \end{aligned}$$

Expanding the product and cancelling the matched leading term,

$$f_{\theta_{\text{eff}}}(z) - f_{\bar{\theta}_{\text{eff}}(c)}(z) = c^{-1}\bar{\mathbf{V}}_{21}^* \hat{\Sigma}(z) \mathbf{U} \tilde{\mathbf{w}} + c\mathbf{W} \hat{\Sigma}(z) \mathbf{P}_{12}^* \tilde{\mathbf{w}} + \mathbf{W} \hat{\Sigma}(z) \mathbf{U} \tilde{\mathbf{w}}.$$

We now identify the first two terms with the trajectory statistics $\mathbf{R}(z)$ and $\mathbf{b}(z)$. Since $\bar{\mathbf{V}}_{21}^* = [\alpha \mathbf{I}_d \quad \mathbf{0}_{d \times d} \quad \mathbf{0}_{d \times 1}]$, we have $\bar{\mathbf{V}}_{21}^* \mathbf{x}_i = \alpha \phi_i$, so

$$\bar{\mathbf{V}}_{21}^* \hat{\Sigma}(z) = \frac{1}{n} \sum_{i=0}^{n-1} (\bar{\mathbf{V}}_{21}^* \mathbf{x}_i) \mathbf{x}_i^\top = \frac{\alpha}{n} \sum_{i=0}^{n-1} \phi_i \mathbf{x}_i^\top = \alpha \mathbf{R}(z).$$

Similarly, $\mathbf{P}_{12}^* \tilde{\mathbf{w}} = [-\mathbf{w}; \mathbf{w}; 1]$, hence $\mathbf{x}_i^\top \mathbf{P}_{12}^* \tilde{\mathbf{w}} = -\phi_i^\top \mathbf{w} + \gamma(\phi_i^+)^\top \mathbf{w} + r_{i+1} = \delta_i$, so

$$\hat{\Sigma}(z) \mathbf{P}_{12}^* \tilde{\mathbf{w}} = \frac{1}{n} \sum_{i=0}^{n-1} \mathbf{x}_i (\mathbf{x}_i^\top \mathbf{P}_{12}^* \tilde{\mathbf{w}}) = \frac{1}{n} \sum_{i=0}^{n-1} \mathbf{x}_i \delta_i = \mathbf{b}(z).$$

Substituting these identities,

$$\begin{aligned} f_{\theta_{\text{eff}}}(z) - f_{\hat{\theta}_{\text{eff}}(c)}(z) &= c^{-1} \alpha \mathbf{R}(z) \mathbf{U} \tilde{\mathbf{w}} + c \mathbf{W} \mathbf{b}(z) + \mathbf{W} \hat{\Sigma}(z) \mathbf{U} \tilde{\mathbf{w}} \\ &=: \mathbf{X}(z) + \mathbf{Y}(z), \end{aligned} \quad (21)$$

where

$$\mathbf{X}(z) := c^{-1} \alpha \mathbf{R}(z) \mathbf{U} \tilde{\mathbf{w}} + c \mathbf{W} \mathbf{b}(z), \quad \mathbf{Y}(z) := \mathbf{W} \hat{\Sigma}(z) \mathbf{U} \tilde{\mathbf{w}}.$$

Step 2: Lower bound on $\|\mathbf{X}\|_{L^2}$. We first lower-bound the two summands of $\mathbf{X}(z)$ separately. Expanding the squared norm and conditioning on $\tilde{\mathbf{w}}$,

$$\begin{aligned} \mathbb{E}_z \|\mathbf{R}(z) \mathbf{U} \tilde{\mathbf{w}}\|^2 &= \mathbb{E}_z [\tilde{\mathbf{w}}^\top \mathbf{U}^\top \mathbf{R}(z)^\top \mathbf{R}(z) \mathbf{U} \tilde{\mathbf{w}}] \\ &= \mathbb{E}_z [\tilde{\mathbf{w}}^\top \mathbf{U}^\top \mathbb{E}[\mathbf{R}(z)^\top \mathbf{R}(z) \mid \tilde{\mathbf{w}}] \mathbf{U} \tilde{\mathbf{w}}] \\ &\geq \kappa_R \mathbb{E}_z \|\mathbf{U} \tilde{\mathbf{w}}\|^2 \\ &= \kappa_R \text{tr}(\mathbf{U} \mathbb{E}_z [\tilde{\mathbf{w}} \tilde{\mathbf{w}}^\top] \mathbf{U}^\top) \\ &\geq \kappa_R \kappa_{\tilde{\mathbf{w}}} \|\mathbf{U}\|_F^2, \end{aligned} \quad (22)$$

where the third line uses Assumption 1 (3), and the last inequality uses Assumption 1 (2). Similarly,

$$\begin{aligned} \mathbb{E}_z \|\mathbf{W} \mathbf{b}(z)\|^2 &= \mathbb{E}_z [\mathbf{b}(z)^\top \mathbf{W}^\top \mathbf{W} \mathbf{b}(z)] \\ &= \mathbb{E}_z [\text{tr}(\mathbf{W} \mathbf{b}(z) \mathbf{b}(z)^\top \mathbf{W}^\top)] \\ &= \text{tr}(\mathbf{W} \mathbb{E}_z [\mathbf{b}(z) \mathbf{b}(z)^\top] \mathbf{W}^\top) \\ &\geq \kappa_q \text{tr}(\mathbf{W} \mathbf{W}^\top) \\ &= \kappa_q \|\mathbf{W}\|_F^2, \end{aligned} \quad (23)$$

where the fourth line uses Assumption 1 (4). Set $A := \mathbb{E}_z \|c^{-1} \alpha \mathbf{R}(z) \mathbf{U} \tilde{\mathbf{w}}\|^2$ and $B := \mathbb{E}_z \|c \mathbf{W} \mathbf{b}(z)\|^2$. Assumption 1 (5) bounds the cross term as

$$|2\mathbb{E}_z \langle c^{-1} \alpha \mathbf{R}(z) \mathbf{U} \tilde{\mathbf{w}}, c \mathbf{W} \mathbf{b}(z) \rangle| \leq 2\rho \sqrt{AB},$$

so expanding $\|\mathbf{X}(z)\|^2$ and applying the cross-term bound,

$$\begin{aligned} \mathbb{E}_z \|\mathbf{X}(z)\|^2 &= A + B + 2\mathbb{E}_z \langle c^{-1} \alpha \mathbf{R}(z) \mathbf{U} \tilde{\mathbf{w}}, c \mathbf{W} \mathbf{b}(z) \rangle \\ &\geq A + B - 2\rho \sqrt{AB} \\ &= (1 - \rho)(A + B) + \rho(\sqrt{A} - \sqrt{B})^2 \\ &\geq (1 - \rho)(A + B), \end{aligned} \quad (24)$$

The two summands A, B are bounded below using the bounds (22) (23) and $|c| \in [c_-, c_+]$:

$$\begin{aligned} A &= c^{-2} \alpha^2 \mathbb{E}_z \|\mathbf{R}(z) \mathbf{U} \tilde{\mathbf{w}}\|^2 \geq c^{-2} \alpha^2 \kappa_R \kappa_{\tilde{\mathbf{w}}} \|\mathbf{U}\|_F^2 \geq c_+^{-2} \alpha^2 \kappa_R \kappa_{\tilde{\mathbf{w}}} \|\mathbf{U}\|_F^2, \\ B &= c^2 \mathbb{E}_z \|\mathbf{W} \mathbf{b}(z)\|^2 \geq c_-^2 \kappa_q \|\mathbf{W}\|_F^2 \geq c_-^2 \kappa_q \|\mathbf{W}\|_F^2. \end{aligned}$$

Plugging into (24), with $\|\Delta\|^2 = \|\mathbf{U}\|_F^2 + \|\mathbf{W}\|_F^2$,

$$\begin{aligned} \mathbb{E}_z \|\mathbf{X}(z)\|^2 &\geq (1 - \rho)(c_+^{-2} \alpha^2 \kappa_R \kappa_{\tilde{\mathbf{w}}} \|\mathbf{U}\|_F^2 + c_-^2 \kappa_q \|\mathbf{W}\|_F^2) \\ &\geq (1 - \rho) \min\{c_+^{-2} \alpha^2 \kappa_R \kappa_{\tilde{\mathbf{w}}}, c_-^2 \kappa_q\} (\|\mathbf{U}\|_F^2 + \|\mathbf{W}\|_F^2) \\ &= m_0 \|\Delta\|^2. \end{aligned}$$

Hence

$$\|\mathbf{X}\|_{L^2} \geq \sqrt{m_0} \|\Delta\|. \quad (25)$$

Step 3: Upper bounds on $\|\mathbf{X}\|_{L^2}$ and $\|\mathbf{Y}\|_{L^2}$. By Assumption 1 (1),

$$\|\mathbf{x}_i\|^2 = \|\phi_i\|^2 + \gamma^2 \|\phi_i^+\|^2 + r_{i+1}^2 \leq 2B_\phi^2 + B_r^2 = B_\Sigma,$$

hence, applying the triangle inequality to $\hat{\Sigma}(z) = \frac{1}{n} \sum_{i=0}^{n-1} \mathbf{x}_i \mathbf{x}_i^\top$,

$$\|\hat{\Sigma}(z)\|_{\text{op}} \leq \frac{1}{n} \sum_{i=0}^{n-1} \|\mathbf{x}_i \mathbf{x}_i^\top\|_{\text{op}} = \frac{1}{n} \sum_{i=0}^{n-1} \|\mathbf{x}_i\|^2 \leq B_\Sigma.$$

Writing $\phi_i = \mathbf{S} \mathbf{x}_i$ with $\mathbf{S} = [\mathbf{I}_d, \mathbf{0}_{d \times d}, \mathbf{0}_{d \times 1}] \in \mathbb{R}^{d \times (2d+1)}$, we have

$$\mathbf{R}(z) = \frac{1}{n} \sum_i \mathbf{S} \mathbf{x}_i \mathbf{x}_i^\top = \mathbf{S} \hat{\Sigma}(z),$$

and $\mathbf{S} \mathbf{S}^\top = \mathbf{I}_d$ gives $\|\mathbf{S}\|_{\text{op}} = 1$. Submultiplicativity then yields

$$\begin{aligned} \|\mathbf{R}(z)\|_{\text{op}} &= \|\mathbf{S} \hat{\Sigma}(z)\|_{\text{op}} \\ &\leq \|\mathbf{S}\|_{\text{op}} \|\hat{\Sigma}(z)\|_{\text{op}} \\ &\leq B_\Sigma. \end{aligned}$$

Also $\|\tilde{\mathbf{w}}\| \leq B_{\tilde{\mathbf{w}}}$. Since $\mathbf{P}_{12}^{\star\top} \mathbf{P}_{12}^\star = \text{diag}(1, 2\mathbf{I}_d)$, $\|\mathbf{P}_{12}^\star\|_{\text{op}} = \sqrt{2}$, hence

$$\begin{aligned} \|\mathbf{b}(z)\| &\leq \|\mathbf{P}_{12}^\star\|_{\text{op}} \|\hat{\Sigma}(z)\|_{\text{op}} \|\tilde{\mathbf{w}}\| \\ &\leq \sqrt{2} B_\Sigma B_{\tilde{\mathbf{w}}}. \end{aligned}$$

By the triangle inequality and submultiplicativity,

$$\begin{aligned} \|\mathbf{X}\|_{L^2} &\leq \|c^{-1} \alpha \mathbf{R}(z) \mathbf{U} \tilde{\mathbf{w}}\|_{L^2} + \|c \mathbf{W} \mathbf{b}(z)\|_{L^2} \\ &\leq |c|^{-1} \alpha \|\mathbf{R}(z)\|_{\text{op}} \|\mathbf{U}\|_{\text{op}} \|\tilde{\mathbf{w}}\| + |c| \|\mathbf{W}\|_{\text{op}} \|\mathbf{b}(z)\| \\ &\leq c_-^{-1} \alpha B_\Sigma B_{\tilde{\mathbf{w}}} \|\mathbf{U}\|_F + \sqrt{2} c_+ B_\Sigma B_{\tilde{\mathbf{w}}} \|\mathbf{W}\|_F. \end{aligned}$$

Applying Cauchy–Schwarz to the right-hand side,

$$\|\mathbf{X}\|_{L^2} \leq B_\Sigma B_{\tilde{\mathbf{w}}} \sqrt{c_-^{-2} \alpha^2 + 2c_+^2} \sqrt{\|\mathbf{U}\|_F^2 + \|\mathbf{W}\|_F^2} \quad (26)$$

$$= \sqrt{M_0} \|\Delta\|. \quad (27)$$

For the quadratic term,

$$\begin{aligned} \|\mathbf{Y}(z)\| &= \|\mathbf{W} \hat{\Sigma}(z) \mathbf{U} \tilde{\mathbf{w}}\| \\ &\leq \|\mathbf{W}\|_{\text{op}} \|\hat{\Sigma}(z)\|_{\text{op}} \|\mathbf{U}\|_{\text{op}} \|\tilde{\mathbf{w}}\| \\ &\leq B_\Sigma B_{\tilde{\mathbf{w}}} \|\mathbf{U}\|_F \|\mathbf{W}\|_F \\ &\leq B_\Sigma B_{\tilde{\mathbf{w}}} \left(\frac{1}{2} \|\mathbf{U}\|_F^2 + \frac{1}{2} \|\mathbf{W}\|_F^2 \right) \\ &= C_Q \|\Delta\|^2. \end{aligned}$$

Thus

$$\|\mathbf{Y}\|_{L^2} \leq C_Q \|\Delta\|^2. \quad (28)$$

Step 4: Excess-loss upper bound. By (20), (21), and (26)–(28),

$$\begin{aligned} \mathcal{L}(\boldsymbol{\theta}_{\text{eff}}) - \mathcal{L}^\star &= \frac{1}{2} \|\mathbf{X} + \mathbf{Y}\|_{L^2}^2 \\ &\leq \frac{1}{2} (\sqrt{M_0} \|\Delta\| + C_Q \|\Delta\|^2)^2 \\ &\leq \frac{1}{2} (\sqrt{M_0} + C_Q r)^2 \|\Delta\|^2, \end{aligned} \quad (29)$$

where the last line uses $\|\Delta\| \leq r$.

Step 5: Directional derivative lower bound. Define

$$g(t) := \mathcal{L}(\bar{\boldsymbol{\theta}}_{\text{eff}}(c) + t\Delta).$$

By the chain rule,

$$g'(1) = \langle \nabla \mathcal{L}(\boldsymbol{\theta}_{\text{eff}}), \Delta \rangle,$$

so Cauchy–Schwarz gives

$$\|\nabla \mathcal{L}(\boldsymbol{\theta}_{\text{eff}})\| \|\Delta\| \geq g'(1). \quad (30)$$

Thus, to establish the PL inequality, it suffices to lower-bound $g'(1)$ with respect to $\|\Delta\|^2$. We now compute $g'(1)$. Replacing $\Delta = (\mathbf{U}, \mathbf{W})$ by $t\Delta = (t\mathbf{U}, t\mathbf{W})$ in the decomposition (21),

$$\begin{aligned} f_{\bar{\boldsymbol{\theta}}_{\text{eff}}(c)+t\Delta}(z) - f_{\bar{\boldsymbol{\theta}}_{\text{eff}}(c)}(z) &= c^{-1}\alpha \mathbf{R}(z)(t\mathbf{U})\tilde{\mathbf{w}} + c(t\mathbf{W})\mathbf{b}(z) + (t\mathbf{W})\hat{\boldsymbol{\Sigma}}(z)(t\mathbf{U})\tilde{\mathbf{w}} \\ &= t[c^{-1}\alpha \mathbf{R}(z)\mathbf{U}\tilde{\mathbf{w}} + c\mathbf{W}\mathbf{b}(z)] + t^2 \mathbf{W}\hat{\boldsymbol{\Sigma}}(z)\mathbf{U}\tilde{\mathbf{w}} \\ &= t\mathbf{X}(z) + t^2\mathbf{Y}(z), \end{aligned}$$

hence

$$g(t) = \frac{1}{2}\mathbb{E}_z \|t\mathbf{X}(z) + t^2\mathbf{Y}(z)\|^2.$$

Differentiating and evaluating at $t = 1$,

$$\begin{aligned} g'(1) &= \|\mathbf{X}\|_{L^2}^2 + 3\mathbb{E}_z \langle \mathbf{X}(z), \mathbf{Y}(z) \rangle + 2\|\mathbf{Y}\|_{L^2}^2 \\ &\geq \|\mathbf{X}\|_{L^2}^2 - 3\|\mathbf{X}\|_{L^2}\|\mathbf{Y}\|_{L^2}. \end{aligned}$$

Set $u := \|\mathbf{X}\|_{L^2}$ and $v := \|\mathbf{Y}\|_{L^2}$. The hypothesis $r < \sqrt{m_0}/(3C_Q)$ together with (25) and (28) gives

$$u \geq \sqrt{m_0}\|\Delta\| > 3C_Q\|\Delta\|^2 \geq 3v,$$

so $u \mapsto u^2 - 3uv$ is increasing at u . Substituting the lower bound on \mathbf{u} (25) and upper bound on \mathbf{v} (28),

$$\begin{aligned} g'(1) &\geq u^2 - 3uv \\ &\geq m_0\|\Delta\|^2 - 3C_Q\sqrt{m_0}\|\Delta\|^3 \\ &\geq m_0\|\Delta\|^2 - 3C_Q\sqrt{m_0}r\|\Delta\|^2 \\ &= (m_0 - 3C_Q\sqrt{m_0}r)\|\Delta\|^2. \end{aligned} \quad (31)$$

Step 6: PL inequality. Combining (30) with (31),

$$\|\nabla \mathcal{L}(\boldsymbol{\theta}_{\text{eff}})\| \|\Delta\| \geq g'(1) \geq (m_0 - 3C_Q\sqrt{m_0}r)\|\Delta\|^2.$$

Squaring (and using (29) to convert $\|\Delta\|^2$ into the excess loss),

$$\frac{1}{2}\|\nabla \mathcal{L}(\boldsymbol{\theta}_{\text{eff}})\|^2 \geq \frac{(m_0 - 3C_Q\sqrt{m_0}r)^2}{(\sqrt{M_0} + C_Qr)^2} (\mathcal{L}(\boldsymbol{\theta}_{\text{eff}}) - \mathcal{L}^*) = \mu_r (\mathcal{L}(\boldsymbol{\theta}_{\text{eff}}) - \mathcal{L}^*),$$

which is the claimed PL inequality on $\mathcal{T}_r(I)$. \square

E Proof of Theorem 3.1

Proof. We construct $\boldsymbol{\theta}^* = (\mathbf{P}^*, \mathbf{V}^*)$ explicitly in four steps: (i) reduce the readout to four blocks of $\boldsymbol{\theta}$; (ii) cancel the cubic-in- \mathbf{w} contribution; (iii) match the affine contribution to the SARSA target; (iv) assemble $\boldsymbol{\theta}^*$ and verify its scaling invariance.

Step 1: Reduction to $\bar{\mathbf{V}}_{21}, \bar{\mathbf{V}}_{22}, \mathbf{P}_{12}, \mathbf{P}_{22}$. Partition \mathbf{V}, \mathbf{P} as in (8), conformal with $D = (2d + 1) + (d + 1)$, and write $\tilde{\mathbf{w}} = [1; \mathbf{w}] \in \mathbb{R}^{d+1}$. Let $\bar{\mathbf{V}}_{21}, \bar{\mathbf{V}}_{22}$ denote the last d rows of $\mathbf{V}_{21}, \mathbf{V}_{22}$, respectively. By Lemma C.1, the transformer update increment simplifies to

$$\Delta \mathbf{w}_{\text{TF}}(\boldsymbol{\theta}) := \text{TF}_{\boldsymbol{\theta}}(\mathbf{H}) - \mathbf{w} = \bar{\mathbf{V}}_{21} \hat{\boldsymbol{\Sigma}} \mathbf{P}_{12} \tilde{\mathbf{w}} + \frac{1}{n} \bar{\mathbf{V}}_{22} \tilde{\mathbf{w}} \tilde{\mathbf{w}}^\top \mathbf{P}_{22} \tilde{\mathbf{w}}, \quad (32)$$

where $\hat{\boldsymbol{\Sigma}} \in \mathbb{R}^{(2d+1) \times (2d+1)}$ is the empirical second-moment matrix of the trajectory features, with the block decomposition

$$\begin{aligned} \hat{\boldsymbol{\Sigma}} &= \begin{bmatrix} \frac{\sum_{i=0}^{n-1} \phi(s_i, a_i) \phi(s_i, a_i)^\top}{n} & \frac{\sum_{i=0}^{n-1} \gamma \phi(s_i, a_i) \phi(s_{i+1}, a_{i+1})^\top}{n} & \frac{\sum_{i=0}^{n-1} r_{i+1} \phi(s_i, a_i)}{n} \\ \frac{\sum_{i=0}^{n-1} \gamma \phi(s_{i+1}, a_{i+1}) \phi(s_i, a_i)^\top}{n} & \frac{\sum_{i=0}^{n-1} \gamma^2 \phi(s_{i+1}, a_{i+1}) \phi(s_{i+1}, a_{i+1})^\top}{n} & \frac{\sum_{i=0}^{n-1} \gamma r_{i+1} \phi(s_{i+1}, a_{i+1})}{n} \\ \frac{\sum_{i=0}^{n-1} r_{i+1} \phi(s_i, a_i)^\top}{n} & \frac{\sum_{i=0}^{n-1} \gamma r_{i+1} \phi(s_{i+1}, a_{i+1})^\top}{n} & \frac{\sum_{i=0}^{n-1} r_{i+1}^2}{n} \end{bmatrix} \\ &:= \begin{bmatrix} \hat{\boldsymbol{\Sigma}}_{\phi\phi} & \gamma \hat{\boldsymbol{\Sigma}}_{\phi\phi_+} & \hat{\boldsymbol{\Sigma}}_{\phi r} \\ \gamma \hat{\boldsymbol{\Sigma}}_{\phi_+\phi} & \gamma^2 \hat{\boldsymbol{\Sigma}}_{\phi_+\phi_+} & \gamma \hat{\boldsymbol{\Sigma}}_{\phi_+ r} \\ \hat{\boldsymbol{\Sigma}}_{r\phi} & \gamma \hat{\boldsymbol{\Sigma}}_{r\phi_+} & \hat{\boldsymbol{\Sigma}}_{rr} \end{bmatrix}. \end{aligned}$$

In particular, the blocks $\mathbf{V}_{11}, \mathbf{V}_{12}, \mathbf{P}_{11}, \mathbf{P}_{21}$ and the first rows of $\mathbf{V}_{21}, \mathbf{V}_{22}$ do not enter the readout, so they are unconstrained.

Step 2: Cancel the cubic term. The batch SARSA update increment (2) can be written compactly as

$$\Delta \mathbf{w}_{\text{SARSA}} = \alpha [\hat{\boldsymbol{\Sigma}}_{\phi r} + \gamma \hat{\boldsymbol{\Sigma}}_{\phi\phi_+} \mathbf{w} - \hat{\boldsymbol{\Sigma}}_{\phi\phi} \mathbf{w}], \quad (33)$$

which is affine in \mathbf{w} . The first term in (32) is also affine via $\tilde{\mathbf{w}} = [1; \mathbf{w}]$, while the second is cubic in \mathbf{w} . Enforcing $\Delta \mathbf{w}_{\text{TF}} \equiv \Delta \mathbf{w}_{\text{SARSA}}$ for every \mathbf{w} therefore requires the cubic term to vanish, for which we set

$$\bar{\mathbf{V}}_{22}^* = \mathbf{0}, \quad \mathbf{P}_{22}^* = \mathbf{0}.$$

Step 3: Match the affine term. It remains to choose $\bar{\mathbf{V}}_{21}^*, \mathbf{P}_{12}^*$ so that

$$\bar{\mathbf{V}}_{21}^* \hat{\boldsymbol{\Sigma}} \mathbf{P}_{12}^* \tilde{\mathbf{w}} = \alpha [\hat{\boldsymbol{\Sigma}}_{\phi r} + \gamma \hat{\boldsymbol{\Sigma}}_{\phi\phi_+} \mathbf{w} - \hat{\boldsymbol{\Sigma}}_{\phi\phi} \mathbf{w}].$$

Take $\bar{\mathbf{V}}_{21}^*$ to extract the first d rows of $\hat{\boldsymbol{\Sigma}}$ with prefactor α :

$$\bar{\mathbf{V}}_{21}^* = [\alpha \mathbf{I}_d, \mathbf{0}_{d \times d}, \mathbf{0}_{d \times 1}] \quad \Rightarrow \quad \bar{\mathbf{V}}_{21}^* \hat{\boldsymbol{\Sigma}} = \alpha [\hat{\boldsymbol{\Sigma}}_{\phi\phi}, \gamma \hat{\boldsymbol{\Sigma}}_{\phi\phi_+}, \hat{\boldsymbol{\Sigma}}_{\phi r}].$$

The matching condition then reduces to $\mathbf{P}_{12}^* \tilde{\mathbf{w}} = [-\mathbf{w}; \mathbf{w}; 1]$, which holds for every $\mathbf{w} \in \mathbb{R}^d$ when

$$\mathbf{P}_{12}^* = \begin{bmatrix} \mathbf{0}_{d \times 1} & -\mathbf{I}_d \\ \mathbf{0}_{d \times 1} & \mathbf{I}_d \\ 1 & \mathbf{0}_{1 \times d} \end{bmatrix}.$$

Step 4: Assembly and scaling. Leave the unconstrained blocks identified in Step 1 as arbitrary entries (denoted $*$). This yields the structure $(\mathbf{P}^*, \mathbf{V}^*)$ in (5), and by construction

$$\text{TF}_{\boldsymbol{\theta}^*}(\mathbf{H}) = \mathbf{w} + \Delta \mathbf{w}_{\text{SARSA}}.$$

Finally, both terms in (32) are bilinear in (\mathbf{V}, \mathbf{P}) , so the rescaled pair $(c\mathbf{P}^*, c^{-1}\mathbf{V}^*)$ produces the same readout for every $c \neq 0$, completing the construction. \square

F Proof of Proposition 3.1

Proof. Let $\boldsymbol{\delta}(\boldsymbol{\theta}, z) := \text{TF}_{\boldsymbol{\theta}}(\mathbf{H}(z)) - \mathbf{w}_{\text{SARSA}}(z)$ denote the per-sample residual, so that

$$\mathcal{L}(\boldsymbol{\theta}) = \frac{1}{2} \mathbb{E}_z \|\boldsymbol{\delta}(\boldsymbol{\theta}, z)\|^2.$$

By Lemma C.1,

$$\boldsymbol{\delta}(\boldsymbol{\theta}, z) = \bar{\mathbf{V}}_{21} \hat{\boldsymbol{\Sigma}}(z) \mathbf{P}_{12} \tilde{\mathbf{w}}(z) + \frac{1}{n} \bar{\mathbf{V}}_{22} \tilde{\mathbf{w}}(z) \tilde{\mathbf{w}}(z)^\top \mathbf{P}_{22} \tilde{\mathbf{w}}(z) + (\mathbf{w}(z) - \mathbf{w}_{\text{SARSA}}(z)), \quad (34)$$

so \mathcal{L} depends on (\mathbf{V}, \mathbf{P}) only through the four sub-blocks $\bar{\mathbf{V}}_{21}, \bar{\mathbf{V}}_{22}, \mathbf{P}_{12}, \mathbf{P}_{22}$.

Part (i). Since $\mathbf{V}_{11}, \mathbf{V}_{12}, \mathbf{P}_{11}, \mathbf{P}_{21}$ do not appear in (34),

$$\nabla_{\mathbf{V}_{11}} \mathcal{L} = \nabla_{\mathbf{V}_{12}} \mathcal{L} = \nabla_{\mathbf{P}_{11}} \mathcal{L} = \nabla_{\mathbf{P}_{21}} \mathcal{L} = \mathbf{0},$$

so each is stationary under the gradient flow (7). For \mathbf{V}_{21} , the loss factors through $\bar{\mathbf{V}}_{21} = \mathbf{S}\mathbf{V}_{21}$ with $\mathbf{S} = [\mathbf{0}_{d \times 1}, \mathbf{I}_d]$, and the chain rule yields

$$\nabla_{\mathbf{V}_{21}} \mathcal{L} = \mathbf{S}^\top \nabla_{\bar{\mathbf{V}}_{21}} \mathcal{L}.$$

Since $\mathbf{S}^\top = [\mathbf{0}_{1 \times d}; \mathbf{I}_d]$ has zero first row, so does $\nabla_{\mathbf{V}_{21}} \mathcal{L}$, and the first row of \mathbf{V}_{21} remains unchanged. The same argument applies to \mathbf{V}_{22} .

Part (ii). A direct computation from (34) gives

$$\nabla_{\bar{\mathbf{V}}_{22}} \mathcal{L}(\boldsymbol{\theta}) = \frac{1}{n} \mathbb{E}_z \left[\boldsymbol{\delta}(\boldsymbol{\theta}, z) (\tilde{\mathbf{w}} \tilde{\mathbf{w}}^\top \mathbf{P}_{22} \tilde{\mathbf{w}})^\top \right], \quad (35)$$

$$\nabla_{\mathbf{P}_{22}} \mathcal{L}(\boldsymbol{\theta}) = \frac{1}{n} \mathbb{E}_z \left[(\boldsymbol{\delta}(\boldsymbol{\theta}, z)^\top \bar{\mathbf{V}}_{22} \tilde{\mathbf{w}}) \tilde{\mathbf{w}} \tilde{\mathbf{w}}^\top \right]. \quad (36)$$

Both (35) and (36) vanish whenever $\mathbf{P}_{22} = \mathbf{0}$ and $\bar{\mathbf{V}}_{22} = \mathbf{0}$. Hence the gradient flow (7) admits a trajectory in which $\mathbf{P}_{22}^{(t)} \equiv \mathbf{0}$ and $\bar{\mathbf{V}}_{22}^{(t)} \equiv \mathbf{0}$, with the remaining blocks evolving freely. \square

G Proof of Theorem 3.2

Proof. We recall the local PL inequality (16) from Lemma C.2: for every $\boldsymbol{\theta}_{\text{eff}} \in \mathcal{T}_r(I)$,

$$\frac{1}{2} \|\nabla \mathcal{L}(\boldsymbol{\theta}_{\text{eff}})\|^2 \geq \mu_r (\mathcal{L}(\boldsymbol{\theta}_{\text{eff}}) - \mathcal{L}^*).$$

We keep the \mathcal{L}^* term explicit for clarity, but it can be dropped since $\mathcal{L}^* = 0$.

Step 1: Bounding the parameter distance to the optimum manifold. Fix any $\boldsymbol{\theta}_{\text{eff}} \in \mathcal{T}_r(I)$ and write its normal decomposition as

$$\boldsymbol{\theta}_{\text{eff}} = \bar{\boldsymbol{\theta}}_{\text{eff}}(c) + \Delta, \quad \Delta = (\mathbf{U}, \mathbf{W}) \in N_c \mathfrak{M}_I, \quad \|\Delta\| < r.$$

As in the proof of Lemma C.2, the residual decomposes as

$$f_{\boldsymbol{\theta}_{\text{eff}}}(z) - f_{\bar{\boldsymbol{\theta}}_{\text{eff}}(c)}(z) = \mathbf{X}(z) + \mathbf{Y}(z),$$

where, by (21),

$$\begin{aligned} \mathbf{X}(z) &:= c^{-1} \alpha \mathbf{R}(z) \mathbf{U} \tilde{\mathbf{w}} + c \mathbf{W} \mathbf{b}(z), \\ \mathbf{Y}(z) &:= \mathbf{W} \hat{\boldsymbol{\Sigma}}(z) \mathbf{U} \tilde{\mathbf{w}}. \end{aligned}$$

By (25),

$$\|\mathbf{X}\|_{L^2} \geq \sqrt{m_0} \|\Delta\|,$$

and by (28),

$$\|\mathbf{Y}\|_{L^2} \leq C_Q \|\Delta\|^2.$$

Therefore, applying the reverse triangle inequality,

$$\begin{aligned} \sqrt{2(\mathcal{L}(\boldsymbol{\theta}_{\text{eff}}) - \mathcal{L}^*)} &= \|\mathbf{X} + \mathbf{Y}\|_{L^2} \\ &\geq \|\mathbf{X}\|_{L^2} - \|\mathbf{Y}\|_{L^2} \\ &\geq (\sqrt{m_0} - C_Q \|\Delta\|) \|\Delta\| \\ &\geq (\sqrt{m_0} - C_Q r) \|\Delta\|, \end{aligned}$$

where the last inequality uses $\|\Delta\| < r$. Squaring both sides,

$$\mathcal{L}(\boldsymbol{\theta}_{\text{eff}}) - \mathcal{L}^* \geq \frac{1}{2} (\sqrt{m_0} - C_Q r)^2 \|\Delta\|^2 = \lambda_r \|\Delta\|^2, \quad (37)$$

where we set

$$\lambda_r := \frac{1}{2}(\sqrt{m_0} - C_Q r)^2.$$

By definition of the tube (10), every point $\boldsymbol{\theta}_{\text{eff}} \in \mathcal{T}_r(I)$ admits a unique normal decomposition

$$\boldsymbol{\theta}_{\text{eff}} = \bar{\boldsymbol{\theta}}_{\text{eff}}(c) + \Delta, \quad \Delta \in N_c \mathfrak{M}_I,$$

so the normal displacement equals the distance to the manifold patch:

$$\|\Delta\| = \text{dist}(\boldsymbol{\theta}_{\text{eff}}, \mathfrak{M}_I).$$

Combining this identity with (37), for all $\boldsymbol{\theta}_{\text{eff}} \in \mathcal{T}_r(I)$,

$$\mathcal{L}(\boldsymbol{\theta}_{\text{eff}}) - \mathcal{L}^* \geq \lambda_r \text{dist}(\boldsymbol{\theta}_{\text{eff}}, \mathfrak{M}_I)^2,$$

and hence

$$\text{dist}(\boldsymbol{\theta}_{\text{eff}}, \mathfrak{M}_I) \leq \frac{1}{\sqrt{\lambda_r}} \sqrt{\mathcal{L}(\boldsymbol{\theta}_{\text{eff}}) - \mathcal{L}^*}. \quad (38)$$

Step 2: Local upper bound on the gradient norm. Define the prediction error

$$\begin{aligned} \mathbf{e}_{\boldsymbol{\theta}_{\text{eff}}}(z) &:= f_{\mathbf{P}_{12}, \bar{\mathbf{V}}_{21}}(z) - f_{\mathbf{P}_{12}^*, \bar{\mathbf{V}}_{21}^*}(z) \\ &= \bar{\mathbf{V}}_{21} \hat{\boldsymbol{\Sigma}}(z) \mathbf{P}_{12} \tilde{\mathbf{w}} - \bar{\mathbf{V}}_{21}^* \hat{\boldsymbol{\Sigma}}(z) \mathbf{P}_{12}^* \tilde{\mathbf{w}}. \end{aligned}$$

Then

$$\mathcal{L}(\boldsymbol{\theta}_{\text{eff}}) - \mathcal{L}^* = \frac{1}{2} \mathbb{E}_z \|\mathbf{e}_{\boldsymbol{\theta}_{\text{eff}}}(z)\|^2,$$

so that

$$\mathbb{E}_z \|\mathbf{e}_{\boldsymbol{\theta}_{\text{eff}}}(z)\|^2 = 2(\mathcal{L}(\boldsymbol{\theta}_{\text{eff}}) - \mathcal{L}^*).$$

Differentiating the bilinear predictor with respect to $\bar{\mathbf{V}}_{21}$ and \mathbf{P}_{12} gives

$$\begin{aligned} \nabla_{\bar{\mathbf{V}}_{21}} \mathcal{L}(\boldsymbol{\theta}_{\text{eff}}) &= \mathbb{E}_z \left[\mathbf{e}_{\boldsymbol{\theta}_{\text{eff}}}(z) (\hat{\boldsymbol{\Sigma}}(z) \mathbf{P}_{12} \tilde{\mathbf{w}})^\top \right], \\ \nabla_{\mathbf{P}_{12}} \mathcal{L}(\boldsymbol{\theta}_{\text{eff}}) &= \mathbb{E}_z \left[\hat{\boldsymbol{\Sigma}}(z)^\top \bar{\mathbf{V}}_{21}^\top \mathbf{e}_{\boldsymbol{\theta}_{\text{eff}}}(z) \tilde{\mathbf{w}}^\top \right]. \end{aligned}$$

For every $\boldsymbol{\theta}_{\text{eff}} \in \mathcal{T}_r(I)$, the triangle inequality together with $\|\Delta\| < r$ yields

$$\begin{aligned} \|\mathbf{P}_{12}\|_F &\leq c_+ \|\mathbf{P}_{12}^*\|_F + r \\ &= c_+ \sqrt{2d+1} + r \\ &=: P_{\max, r}, \end{aligned}$$

and

$$\begin{aligned} \|\bar{\mathbf{V}}_{21}\|_F &\leq c_-^{-1} \|\bar{\mathbf{V}}_{21}^*\|_F + r \\ &= c_-^{-1} \sqrt{d} + r \\ &=: V_{\max, r}. \end{aligned}$$

Moreover, by Assumption 1 (1),

$$\|\hat{\boldsymbol{\Sigma}}(z)\|_{\text{op}} \leq B_\Sigma,$$

and

$$\|\tilde{\mathbf{w}}\| \leq B_{\tilde{w}}.$$

Therefore, by Cauchy–Schwarz and submultiplicativity,

$$\begin{aligned} \|\nabla_{\bar{\mathbf{V}}_{21}} \mathcal{L}(\boldsymbol{\theta}_{\text{eff}})\|_F &\leq B_\Sigma B_{\tilde{w}} P_{\max, r} (\mathbb{E}_z \|\mathbf{e}_{\boldsymbol{\theta}_{\text{eff}}}(z)\|^2)^{1/2} \\ &= \sqrt{2} B_\Sigma B_{\tilde{w}} P_{\max, r} \sqrt{\mathcal{L}(\boldsymbol{\theta}_{\text{eff}}) - \mathcal{L}^*}, \end{aligned}$$

and similarly,

$$\|\nabla_{\mathbf{P}_{12}} \mathcal{L}(\boldsymbol{\theta}_{\text{eff}})\|_F \leq \sqrt{2} B_\Sigma B_{\tilde{w}} V_{\max, r} \sqrt{\mathcal{L}(\boldsymbol{\theta}_{\text{eff}}) - \mathcal{L}^*}.$$

Combining the two estimates and recalling that

$$K_r = \sqrt{2} B_\Sigma B_{\tilde{w}} \sqrt{P_{\max, r}^2 + V_{\max, r}^2},$$

we obtain the gradient upper bound

$$\|\nabla \mathcal{L}(\boldsymbol{\theta}_{\text{eff}})\| \leq K_r \sqrt{\mathcal{L}(\boldsymbol{\theta}_{\text{eff}}) - \mathcal{L}^*}, \quad \forall \boldsymbol{\theta}_{\text{eff}} \in \mathcal{T}_r(I). \quad (39)$$

Step 3: Invariance of the tube. Let $\boldsymbol{\theta}_{\text{eff}}(t)$ denote the maximal solution of the gradient flow (7) starting from $\boldsymbol{\theta}_{\text{eff}}(0)$. Since $\nabla\mathcal{L}$ is locally Lipschitz, a unique local solution exists. Define the exit time

$$\tau := \inf\{t > 0 : \boldsymbol{\theta}_{\text{eff}}(t) \notin \mathcal{T}_r(I)\}.$$

We will show that $\tau = \infty$. For all $t < \tau$, the local PL inequality (16) holds, and along the gradient flow,

$$\begin{aligned} \frac{d}{dt}\mathcal{L}(\boldsymbol{\theta}_{\text{eff}}(t)) &= \langle \nabla\mathcal{L}(\boldsymbol{\theta}_{\text{eff}}(t)), \dot{\boldsymbol{\theta}}_{\text{eff}}(t) \rangle \\ &= -\|\nabla\mathcal{L}(\boldsymbol{\theta}_{\text{eff}}(t))\|^2 \\ &\leq -2\mu_r(\mathcal{L}(\boldsymbol{\theta}_{\text{eff}}(t)) - \mathcal{L}^*). \end{aligned}$$

Since $\mathcal{L}^* = 0$, Gronwall's inequality yields the loss decay bound

$$\mathcal{L}(\boldsymbol{\theta}_{\text{eff}}(t)) - \mathcal{L}^* \leq e^{-2\mu_r t} (\mathcal{L}(\boldsymbol{\theta}_{\text{eff}}(0)) - \mathcal{L}^*), \quad \forall t < \tau. \quad (40)$$

Combining (39) with (40), for every $t < \tau$,

$$\begin{aligned} \|\dot{\boldsymbol{\theta}}_{\text{eff}}(t)\| &= \|\nabla\mathcal{L}(\boldsymbol{\theta}_{\text{eff}}(t))\| \\ &\leq K_r \sqrt{\mathcal{L}(\boldsymbol{\theta}_{\text{eff}}(t)) - \mathcal{L}^*} \\ &\leq K_r \sqrt{\mathcal{L}(\boldsymbol{\theta}_{\text{eff}}(0)) - \mathcal{L}^*} e^{-\mu_r t}. \end{aligned}$$

Integrating, for every $t < \tau$,

$$\begin{aligned} \|\boldsymbol{\theta}_{\text{eff}}(t) - \boldsymbol{\theta}_{\text{eff}}(0)\| &\leq \int_0^t \|\dot{\boldsymbol{\theta}}_{\text{eff}}(s)\| ds \\ &\leq K_r \sqrt{\mathcal{L}(\boldsymbol{\theta}_{\text{eff}}(0)) - \mathcal{L}^*} \int_0^t e^{-\mu_r s} ds \\ &\leq \frac{K_r}{\mu_r} \sqrt{\mathcal{L}(\boldsymbol{\theta}_{\text{eff}}(0)) - \mathcal{L}^*}. \end{aligned} \quad (41)$$

We next upper-bound the initial excess loss in terms of the distance to \mathfrak{M}_{I_0} . From (29), since $\|\Delta\| = \text{dist}(\boldsymbol{\theta}_{\text{eff}}, \mathfrak{M}_I)$ and $\mathfrak{M}_{I_0} \subset \mathfrak{M}_I$,

$$\begin{aligned} \mathcal{L}(\boldsymbol{\theta}_{\text{eff}}) - \mathcal{L}^* &\leq \frac{1}{2}(\sqrt{M_0} + C_Q r)^2 \|\Delta\|^2 \\ &= \frac{1}{2}(\sqrt{M_0} + C_Q r)^2 \text{dist}(\boldsymbol{\theta}_{\text{eff}}, \mathfrak{M}_I)^2 \\ &\leq \frac{1}{2}(\sqrt{M_0} + C_Q r)^2 \text{dist}(\boldsymbol{\theta}_{\text{eff}}, \mathfrak{M}_{I_0})^2. \end{aligned} \quad (42)$$

Combining (41) and (42), for every $t < \tau$,

$$\begin{aligned} \text{dist}(\boldsymbol{\theta}_{\text{eff}}(t), \mathfrak{M}_{I_0}) &\leq \text{dist}(\boldsymbol{\theta}_{\text{eff}}(0), \mathfrak{M}_{I_0}) + \|\boldsymbol{\theta}_{\text{eff}}(t) - \boldsymbol{\theta}_{\text{eff}}(0)\| \\ &\leq \text{dist}(\boldsymbol{\theta}_{\text{eff}}(0), \mathfrak{M}_{I_0}) + \frac{K_r}{\mu_r} \sqrt{\mathcal{L}(\boldsymbol{\theta}_{\text{eff}}(0)) - \mathcal{L}^*} \\ &\leq \text{dist}(\boldsymbol{\theta}_{\text{eff}}(0), \mathfrak{M}_{I_0}) \left(1 + \frac{K_r(\sqrt{M_0} + C_Q r)}{\sqrt{2}\mu_r} \right) \\ &< \eta_{I_0, r}, \end{aligned}$$

where the last inequality follows from the initialization condition (12). By the definition of $\eta_{I_0, r}$ in (11), this implies

$$\boldsymbol{\theta}_{\text{eff}}(t) \in \mathcal{T}_r(I), \quad \forall t < \tau.$$

Hence the solution cannot exit $\mathcal{T}_r(I)$ at any finite time, so $\tau = \infty$.

Step 4: Convergence to the optimum manifold. Since the trajectory is confined to the bounded neighborhood

$$\{\boldsymbol{\theta}_{\text{eff}} \in \Theta_{\text{eff}} : \text{dist}(\boldsymbol{\theta}_{\text{eff}}, \mathfrak{M}_{I_0}) \leq \eta_{I_0, r}\},$$

no finite-time blow-up occurs and the gradient flow is well defined for all $t \geq 0$. The exponential loss decay (40) therefore holds globally:

$$\mathcal{L}(\boldsymbol{\theta}_{\text{eff}}(t)) - \mathcal{L}^* \leq e^{-2\mu_r t} (\mathcal{L}(\boldsymbol{\theta}_{\text{eff}}(0)) - \mathcal{L}^*), \quad \forall t \geq 0. \quad (43)$$

Combining (38) with (43),

$$\begin{aligned} \text{dist}(\boldsymbol{\theta}_{\text{eff}}(t), \mathfrak{M}_I)^2 &\leq \frac{1}{\lambda_r} (\mathcal{L}(\boldsymbol{\theta}_{\text{eff}}(t)) - \mathcal{L}^*) \\ &\leq \frac{1}{\lambda_r} e^{-2\mu_r t} (\mathcal{L}(\boldsymbol{\theta}_{\text{eff}}(0)) - \mathcal{L}^*). \end{aligned} \quad (44)$$

It remains to show that the parameters themselves converge to a point on \mathfrak{M}_I . By the same argument as in (41), for any $0 \leq t_1 < t_2$,

$$\begin{aligned} \|\boldsymbol{\theta}_{\text{eff}}(t_2) - \boldsymbol{\theta}_{\text{eff}}(t_1)\| &\leq \int_{t_1}^{t_2} \|\dot{\boldsymbol{\theta}}_{\text{eff}}(s)\| ds \\ &\leq K_r \sqrt{\mathcal{L}(\boldsymbol{\theta}_{\text{eff}}(0)) - \mathcal{L}^*} \int_{t_1}^{t_2} e^{-\mu_r s} ds \\ &\leq \frac{K_r}{\mu_r} \sqrt{\mathcal{L}(\boldsymbol{\theta}_{\text{eff}}(0)) - \mathcal{L}^*} e^{-\mu_r t_1}. \end{aligned} \quad (45)$$

Hence $\boldsymbol{\theta}_{\text{eff}}(t)$ is a Cauchy curve as $t \rightarrow \infty$. By completeness of Θ_{eff} , there exists $\boldsymbol{\theta}_{\text{eff}}(\infty) \in \Theta_{\text{eff}}$ such that

$$\lim_{t \rightarrow \infty} \boldsymbol{\theta}_{\text{eff}}(t) = \boldsymbol{\theta}_{\text{eff}}(\infty).$$

Letting $t_2 \rightarrow \infty$ in (45),

$$\|\boldsymbol{\theta}_{\text{eff}}(t) - \boldsymbol{\theta}_{\text{eff}}(\infty)\| \leq \frac{K_r}{\mu_r} \sqrt{\mathcal{L}(\boldsymbol{\theta}_{\text{eff}}(0)) - \mathcal{L}^*} e^{-\mu_r t}.$$

By continuity of \mathcal{L} together with (43),

$$\mathcal{L}(\boldsymbol{\theta}_{\text{eff}}(\infty)) = \mathcal{L}^*.$$

Moreover, by (44),

$$\text{dist}(\boldsymbol{\theta}_{\text{eff}}(t), \mathfrak{M}_I) \rightarrow 0 \quad \text{as } t \rightarrow \infty,$$

and since \mathfrak{M}_I is closed, we conclude that

$$\boldsymbol{\theta}_{\text{eff}}(\infty) \in \mathfrak{M}_I.$$

This completes the proof. \square

H Proof of Theorem 3.3

Proof. The argument follows the same four-step structure as the proof of Theorem 3.1; only the dimensions and the affine target change.

Step 1: Reduction. The actor-critic prompt (13) has the same block-diagonal form as the SARSA prompt (4), except the trajectory columns $\mathbf{h}_{i+1} := [\mathbf{x}_i; \mathbf{0}]$, $i = 0, \dots, n-1$ occupy the upper $(2d+m+1)$ -block, while the parameter column $\mathbf{h}_{n+1} = [\mathbf{0}_{2d+m+1}; \tilde{\mathbf{w}}]$ occupies the lower $(d+m+1)$ -block, with

$$\mathbf{x}_i = \begin{bmatrix} \phi_V(s_i) \\ \gamma \phi_V(s_{i+1}) \\ r_{i+1} \\ \gamma^i \mathbf{g}\boldsymbol{\lambda}(s_i, a_i) \end{bmatrix} \in \mathbb{R}^{2d+m+1}, \text{ and } \tilde{\mathbf{w}} = \begin{bmatrix} 1 \\ \boldsymbol{\lambda} \\ \mathbf{w} \end{bmatrix} \in \mathbb{R}^{d+m+1}.$$

Partitioning \mathbf{V}, \mathbf{P} conformally with $D = (2d + m + 1) + (d + m + 1)$ as in (8), and letting $\bar{\mathbf{V}}_{21}, \bar{\mathbf{V}}_{22}$ now denote the *last* $d + m$ rows of $\mathbf{V}_{21}, \mathbf{V}_{22}$, the same block computation as in Lemma C.1 yields

$$\begin{bmatrix} \Delta \lambda_{\text{TF}}(\boldsymbol{\theta}) \\ \Delta \mathbf{w}_{\text{TF}}(\boldsymbol{\theta}) \end{bmatrix} := \text{TF}_{\boldsymbol{\theta}}(\mathbf{H}) - \begin{bmatrix} \boldsymbol{\lambda} \\ \mathbf{w} \end{bmatrix} = \bar{\mathbf{V}}_{21} \hat{\boldsymbol{\Sigma}} \mathbf{P}_{12} \tilde{\mathbf{w}} + \frac{1}{n} \bar{\mathbf{V}}_{22} \tilde{\mathbf{w}} \tilde{\mathbf{w}}^\top \mathbf{P}_{22} \tilde{\mathbf{w}}, \quad (46)$$

where $\hat{\boldsymbol{\Sigma}} \in \mathbb{R}^{(2d+m+1) \times (2d+m+1)}$ is the empirical second-moment matrix of the trajectory features:

$$\hat{\boldsymbol{\Sigma}} = \frac{1}{n} \sum_{i=0}^{n-1} \mathbf{x}_i \mathbf{x}_i^\top := \begin{bmatrix} \hat{\boldsymbol{\Sigma}}_{\phi_V \phi_V} & \gamma \hat{\boldsymbol{\Sigma}}_{\phi_V \phi_{V+}} & \hat{\boldsymbol{\Sigma}}_{\phi_V r} & \hat{\boldsymbol{\Sigma}}_{\phi_V g} \\ \gamma \hat{\boldsymbol{\Sigma}}_{\phi_{V+} \phi_V} & \gamma^2 \hat{\boldsymbol{\Sigma}}_{\phi_{V+} \phi_{V+}} & \gamma \hat{\boldsymbol{\Sigma}}_{\phi_{V+} r} & \gamma \hat{\boldsymbol{\Sigma}}_{\phi_{V+} g} \\ \hat{\boldsymbol{\Sigma}}_{r \phi_V} & \gamma \hat{\boldsymbol{\Sigma}}_{r \phi_{V+}} & \hat{\boldsymbol{\Sigma}}_{rr} & \hat{\boldsymbol{\Sigma}}_{rg} \\ \hat{\boldsymbol{\Sigma}}_{g \phi_V} & \gamma \hat{\boldsymbol{\Sigma}}_{g \phi_{V+}} & \hat{\boldsymbol{\Sigma}}_{gr} & \hat{\boldsymbol{\Sigma}}_{gg} \end{bmatrix}.$$

The blocks $\mathbf{V}_{11}, \mathbf{V}_{12}, \mathbf{P}_{11}, \mathbf{P}_{21}$ and the first row of $\mathbf{V}_{21}, \mathbf{V}_{22}$ are unconstrained.

Step 2: Cancel the cubic term. The actor-critic update (3) can be written as

$$\begin{bmatrix} \Delta \boldsymbol{\lambda}_{\text{AC}} \\ \Delta \mathbf{w}_{\text{AC}} \end{bmatrix} = \begin{bmatrix} \alpha [\hat{\boldsymbol{\Sigma}}_{gr} + \gamma \hat{\boldsymbol{\Sigma}}_{g \phi_{V+}} \mathbf{w} - \hat{\boldsymbol{\Sigma}}_{g \phi_V} \mathbf{w}] \\ \beta [\hat{\boldsymbol{\Sigma}}_{\phi_V r} + \gamma \hat{\boldsymbol{\Sigma}}_{\phi_V \phi_{V+}} \mathbf{w} - \hat{\boldsymbol{\Sigma}}_{\phi_V \phi_V} \mathbf{w}] \end{bmatrix}, \quad (47)$$

which is affine in $(\boldsymbol{\lambda}, \mathbf{w})$. Setting $\bar{\mathbf{V}}_{22}^* = \mathbf{P}_{22}^* = \mathbf{0}$ removes the cubic term in (46).

Step 3: Match the affine term. We require $\bar{\mathbf{V}}_{21}^* \hat{\boldsymbol{\Sigma}} \mathbf{P}_{12}^* \tilde{\mathbf{w}} = [\Delta \boldsymbol{\lambda}_{\text{AC}}; \Delta \mathbf{w}_{\text{AC}}]$ for every $(\boldsymbol{\lambda}, \mathbf{w})$. Take

$$\bar{\mathbf{V}}_{21}^* = \begin{bmatrix} \mathbf{0}_{m \times d} & \mathbf{0}_{m \times d} & \mathbf{0}_{m \times 1} & \alpha \mathbf{I}_m \\ \beta \mathbf{I}_d & \mathbf{0}_{d \times d} & \mathbf{0}_{d \times 1} & \mathbf{0}_{d \times m} \end{bmatrix},$$

which extracts the bottom m rows (prefactor by α), and the top d rows (prefactor by β) of $\hat{\boldsymbol{\Sigma}}$:

$$\bar{\mathbf{V}}_{21}^* \hat{\boldsymbol{\Sigma}} = \begin{bmatrix} \alpha \hat{\boldsymbol{\Sigma}}_{g \phi_V} & \alpha \gamma \hat{\boldsymbol{\Sigma}}_{g \phi_{V+}} & \alpha \hat{\boldsymbol{\Sigma}}_{gr} & \alpha \hat{\boldsymbol{\Sigma}}_{gg} \\ \beta \hat{\boldsymbol{\Sigma}}_{\phi_V \phi_V} & \beta \gamma \hat{\boldsymbol{\Sigma}}_{\phi_V \phi_{V+}} & \beta \hat{\boldsymbol{\Sigma}}_{\phi_V r} & \beta \hat{\boldsymbol{\Sigma}}_{\phi_V g} \end{bmatrix}.$$

The matching condition then reduces to $\mathbf{P}_{12}^* \tilde{\mathbf{w}} = [-\mathbf{w}; \mathbf{w}; 1; \mathbf{0}_m]$. With $\tilde{\mathbf{w}} = [1; \boldsymbol{\lambda}; \mathbf{w}]$, this holds for every $(\boldsymbol{\lambda}, \mathbf{w})$ when

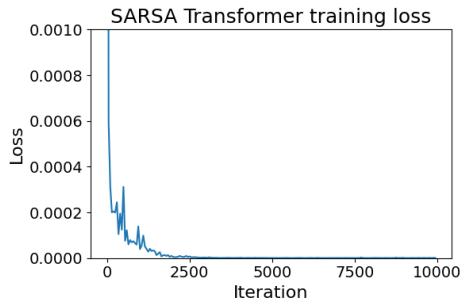
$$\mathbf{P}_{12}^* = \begin{bmatrix} \mathbf{0}_{d \times 1} & \mathbf{0}_{d \times m} & -\mathbf{I}_d \\ \mathbf{0}_{d \times 1} & \mathbf{0}_{d \times m} & \mathbf{I}_d \\ 1 & \mathbf{0}_{1 \times m} & \mathbf{0}_{1 \times d} \\ \mathbf{0}_{m \times 1} & \mathbf{0}_{m \times m} & \mathbf{0}_{m \times d} \end{bmatrix}.$$

Step 4: Assembly and scaling. Leaving the unconstrained blocks as $*$, we recover $(\mathbf{P}^*, \mathbf{V}^*)$ as displayed in (14). Bilinearity of (46) in (\mathbf{V}, \mathbf{P}) gives the same scaling invariance under $(\mathbf{P}^*, \mathbf{V}^*) \mapsto (c\mathbf{P}^*, c^{-1}\mathbf{V}^*)$ for any $c \neq 0$, completing the construction. \square

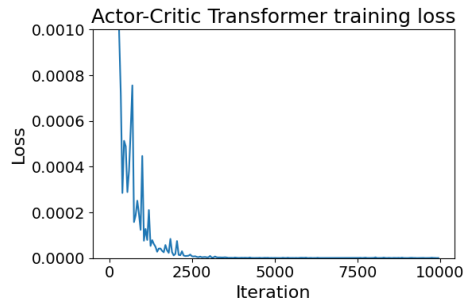
I Additional Experiments

I.1 Training loss curves

We plot the training loss $\hat{\mathcal{L}}(\boldsymbol{\theta}^{(t)})$ over training iterations for both the SARSA transformer and the Actor-Critic transformer in our experiments presented in Section 4. The results are shown in Figure 4.



(a) SARSA transformer.



(b) Actor-Critic transformer.

Figure 4: Training loss $\hat{\mathcal{L}}(\theta^{(t)})$ over training iterations for the SARSA transformer (left) and the Actor-Critic transformer (right). In both settings, the loss decays approximately exponentially to near zero, consistent with the local convergence guarantee in Theorem 3.2.

I.2 Experimental Detail

The trainings and evaluations of the transformers used in our experiment were conducted on a Windows 11 machine with the following specifications:

- GPU: NVIDIA GeForce RTX 4090
- CPU: Intel Core i9-14900KF
- Memory: 32 GB DDR5, 5600MHz

The training procedure takes approximately 20 minutes for the IC-SARSA transformer and 30 minutes for the IC-AC transformer; evaluation takes approximately 5 and 10 minutes, respectively.